

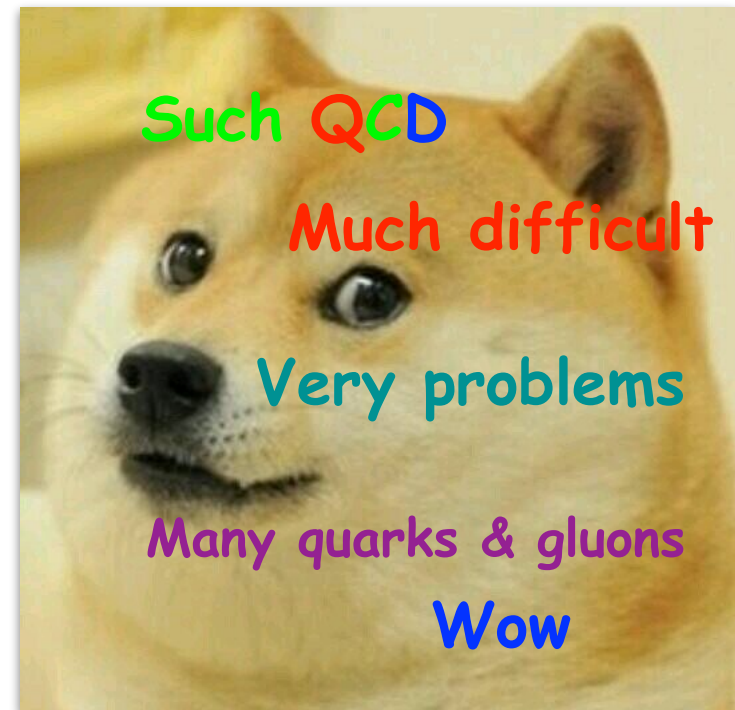
QCD EoS in medium via effective models

Seung-il Nam

Department of Physics, Pukyong National University (PKNU),
Center for Extreme Nuclear Matters (CENuM), Korea University,
Asia Pacific Center for Theoretical Center Physics (APCTP),
Republic of Korea



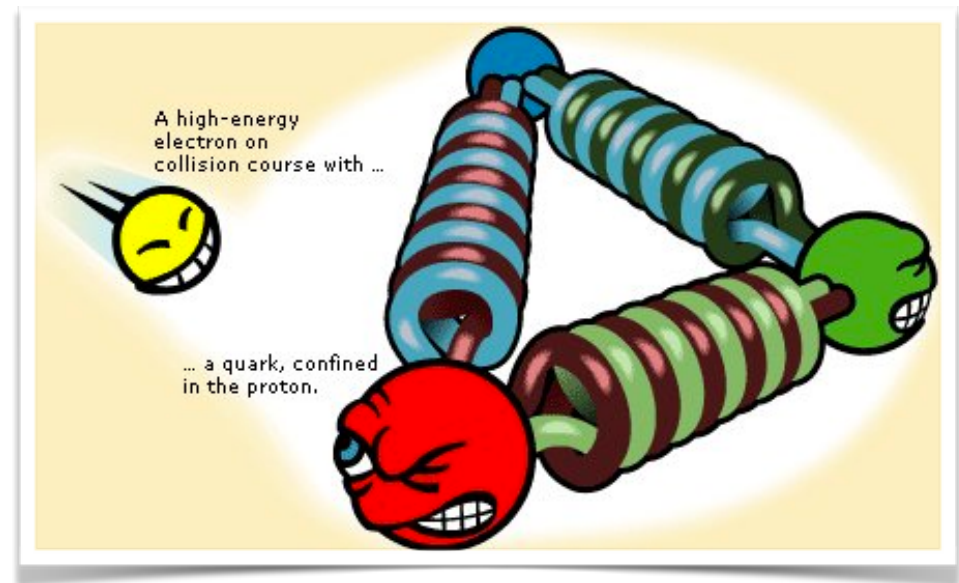
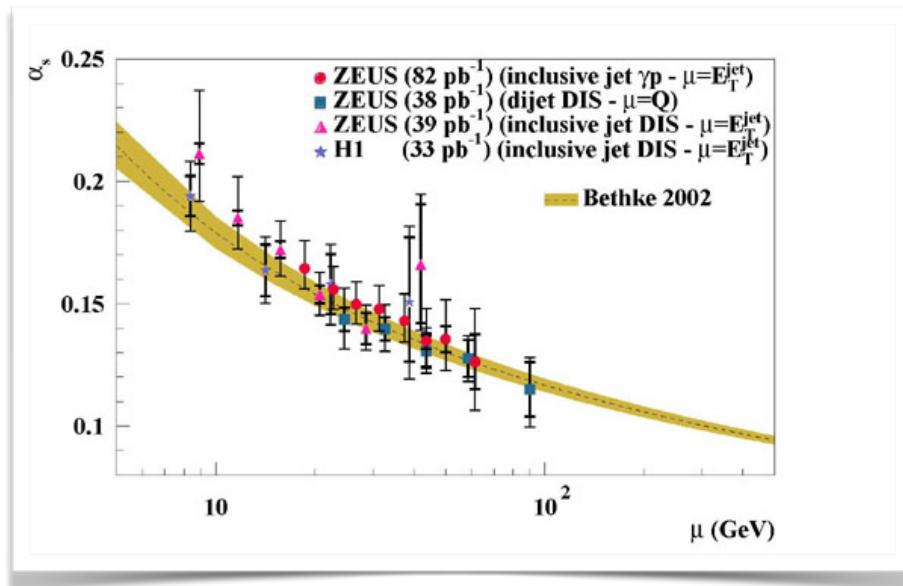
1. Introduction: QCD and effective models
2. QCD at extreme conditions
3. Medium-modified Effective models
4. Some numerical results
5. Summary



1. Introduction: **QCD** and effective models

Strongly interacting particles such as quarks and gluons are governed by **QCD**

Nonlinear interactions of quarks and gluons leads to nontrivial feature of **QCD: Asymptotic freedom** and **Confinement**



Nonperturbative QCD

perturbative QCD



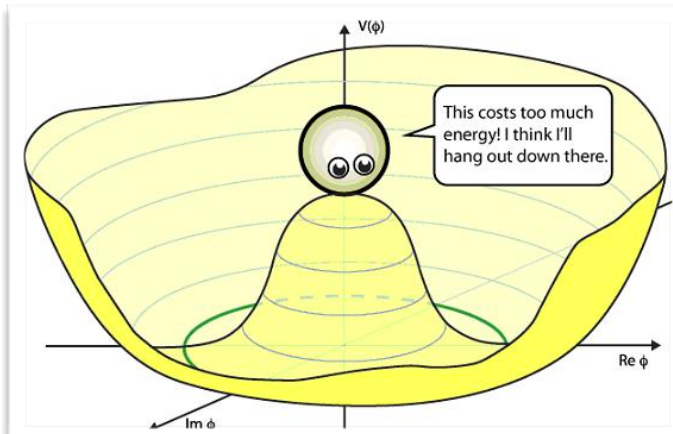
No free quarks observed yet

1. Introduction: QCD and effective models

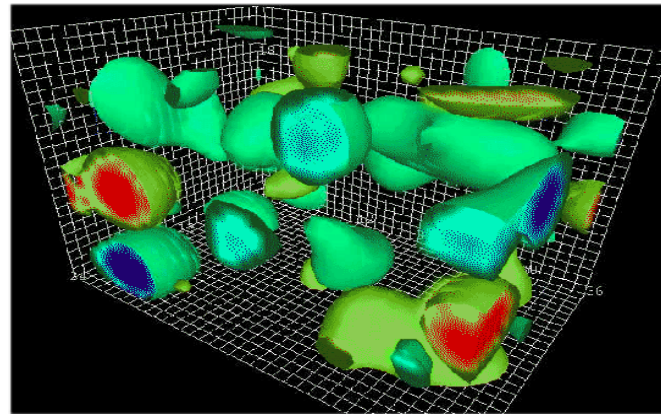
QCD has accumulated many successful interpretations for hadrons, strongly-interacting vacuum, quark matters, perturbative QCD, etc.

Insufficient understandings on low-energy QCD: Mass gap of YM theory

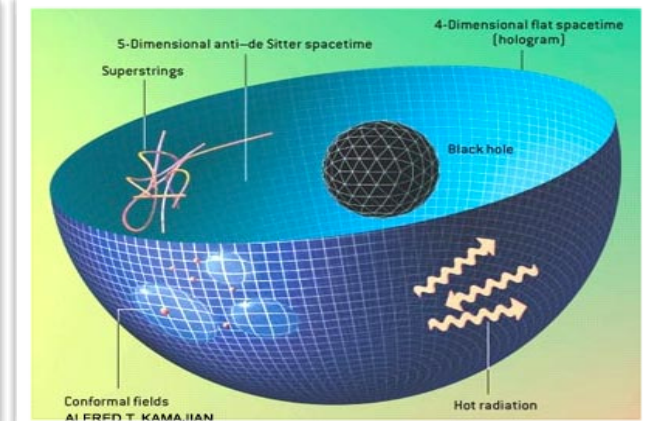
How can we get over this problem?



Relevant symmetries
Effective QCD-like models



Embedding on computer
Lattice QCD



Dualities in space-time
Holographic QCD

1. Introduction: QCD and effective models

Effective models of QCD based on relevant symmetries and their dynamical breakdowns



Being motivated by the superconducting theory,

Nambu and **Jona-Lasinio** suggested an effective model of QCD:
“NJL model”

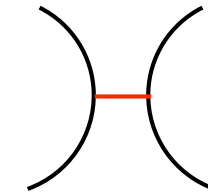
$$L = \bar{\psi} \left[i \gamma_{\mu} \partial^{\mu} - (m_c + \eta) \right] \psi - \delta \eta \bar{\psi} \psi + \delta G_S \left[(\bar{\psi} \psi)^2 + (\bar{\psi} i \gamma_5 \boldsymbol{\tau} \psi)^2 \right],$$

Spontaneous Chiral Symmetry Breaking (SCSB) leads to emergence of pion, dynamical mass for quarks, finite low-energy constant, etc.

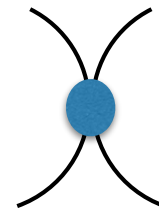
1. Introduction: QCD and effective models

According to SCSB, QCD mutates at low-energy region as

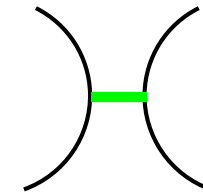
Quark-gluon interactions (QCD)



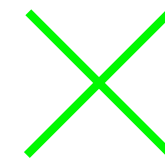
Four-quark (local) interactions (NJL)



Quark-pion interactions (ChQM)



Pure-pion interactions (ChPT)



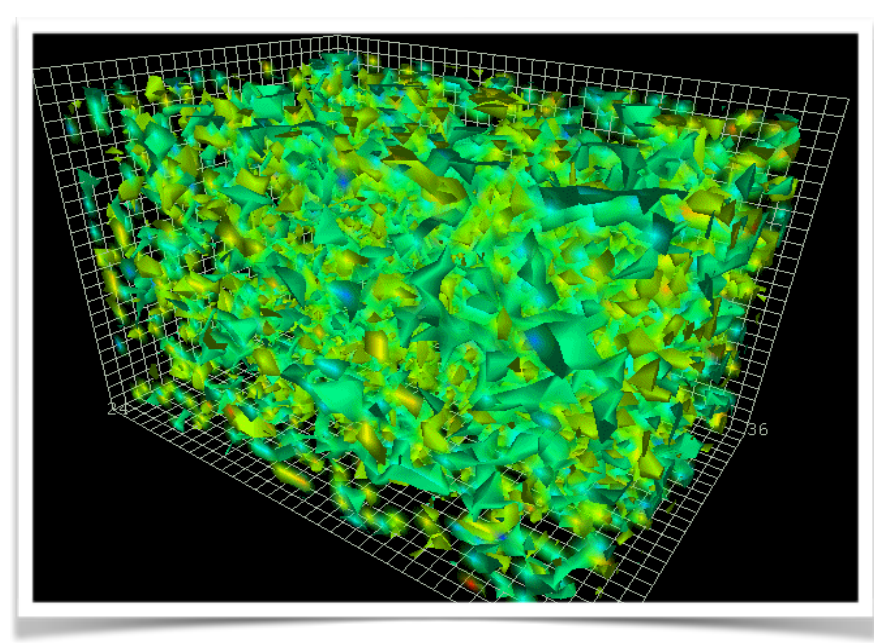
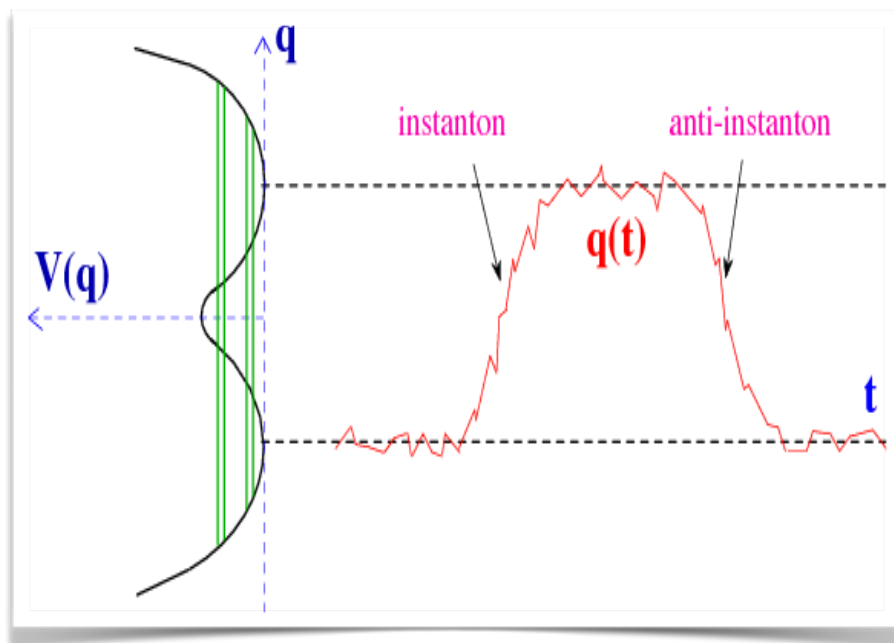
1. Introduction: QCD and effective models

A sophisticated QCD-like model: **Liquid-Instanton Model (LIM)**

Instanton: A semi-classical solution which minimize YM action

Simpler understanding of instanton: Tunneling path of vacua

Or, instanton is a low-energy effective-nonperturbative gluon



1. Introduction: QCD and effective models

Instanton interprets well the spontaneous chiral symmetry breaking (SCSB) and $U(1)$ axial anomaly (Witten-Veneziano theorem), etc.

Technically, it has only two model parameters for light-flavor sector in the large N_c limit: Average instanton size & inter-instanton distance

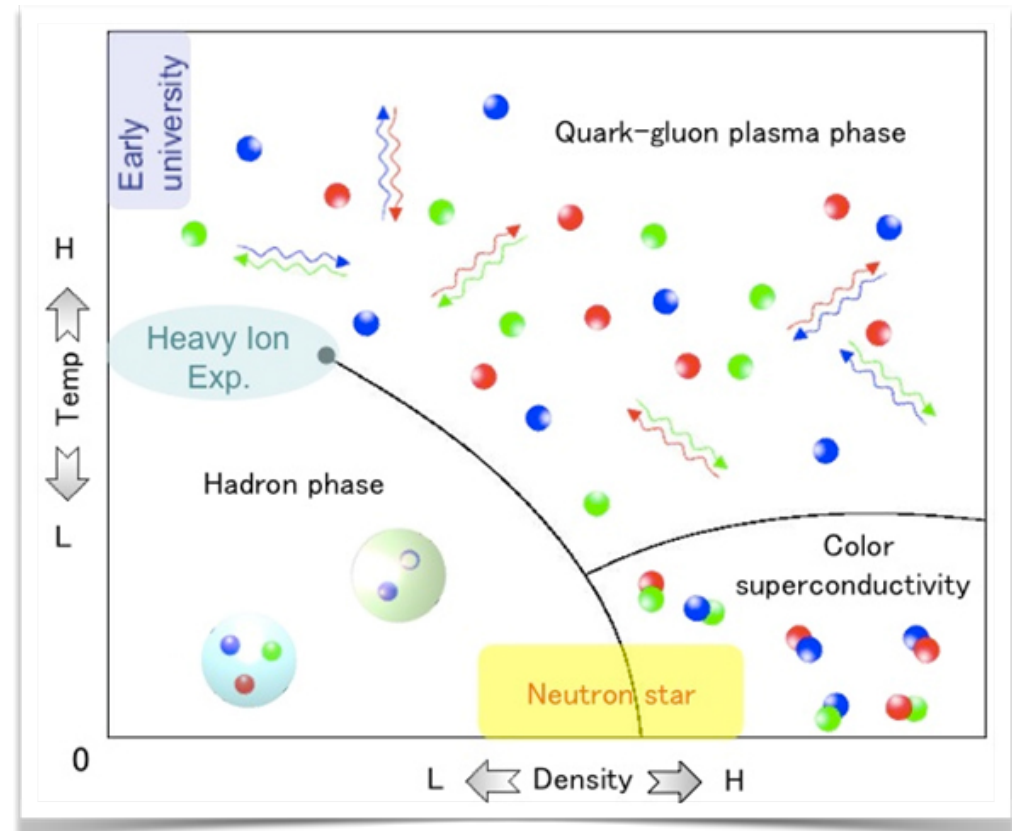
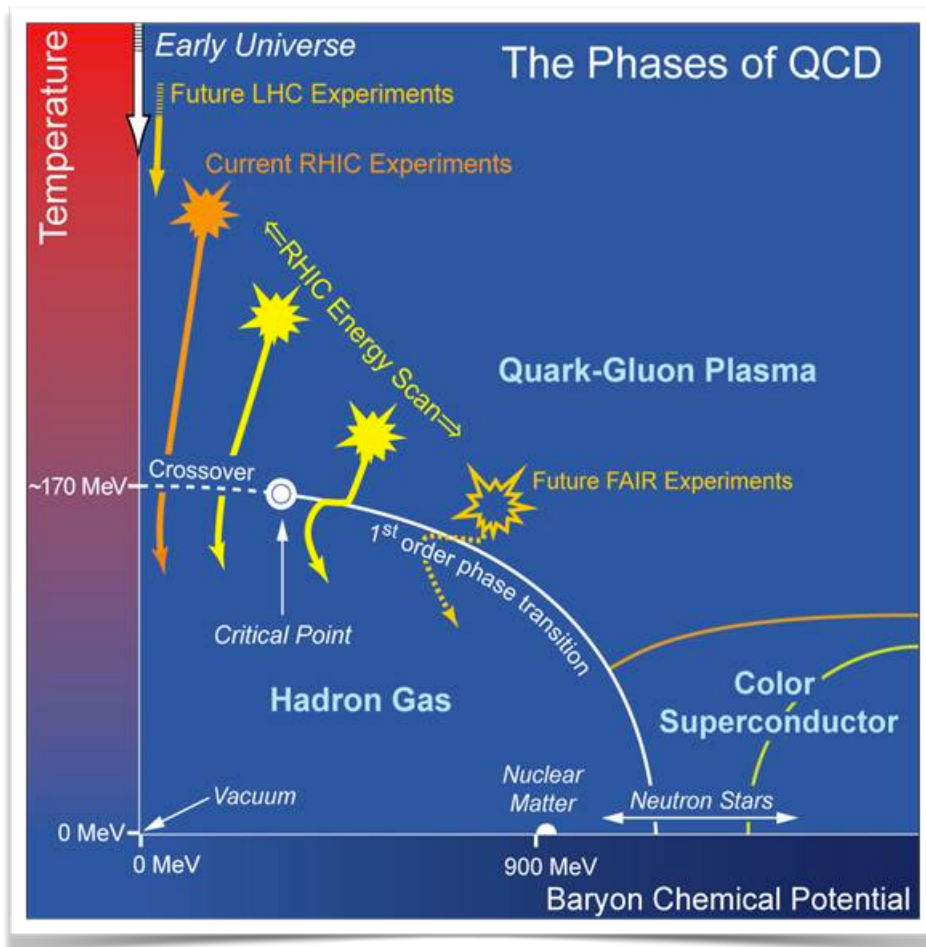
Unfortunately, there is NO confinement!!!

Some suggestions for the confinement with instanton physics:
Dyon, nontrivial-holonomy caloron, etc.

It has been believed that confinement is not so relevant in ground-state hadron spectra, in contrast to resonances, Regge behavior, Hagedorn spectrum, etc.

2. QCD at extreme conditions

QCD has complicated **phase structure** as a function of temperature and density



2. QCD at extreme conditions

- I. Each QCD phases defined by its own order parameters
- II. Behavior of order parameters governed by dynamics of symmetry
- III. Symmetry and its breakdown governed by vacuum structure

Chiral symmetry \leftrightarrow Quark (chiral) condensate: Hadron or not?

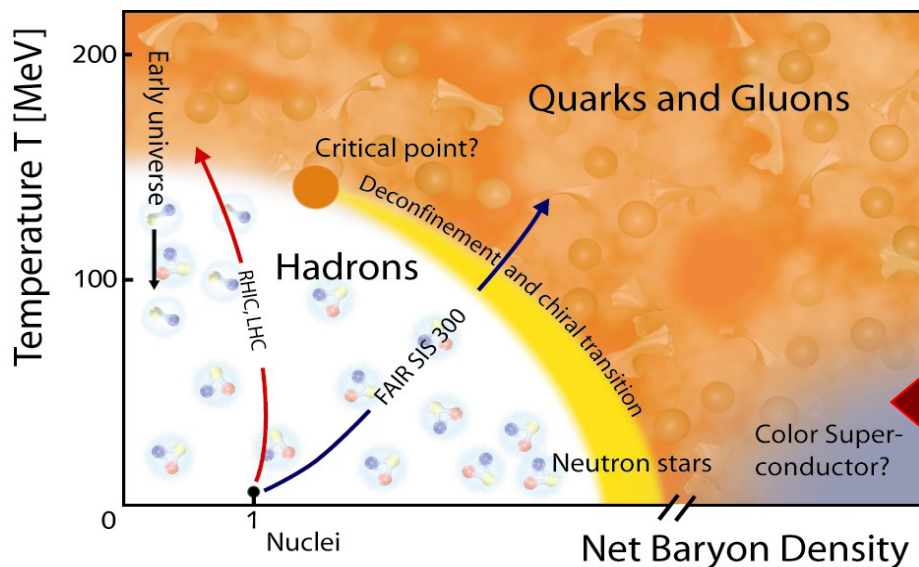
Center symmetry \leftrightarrow VEV of Polyakov loop: Confined or not?

Color symmetry \leftrightarrow Diquark condensate: Superconducting or not?

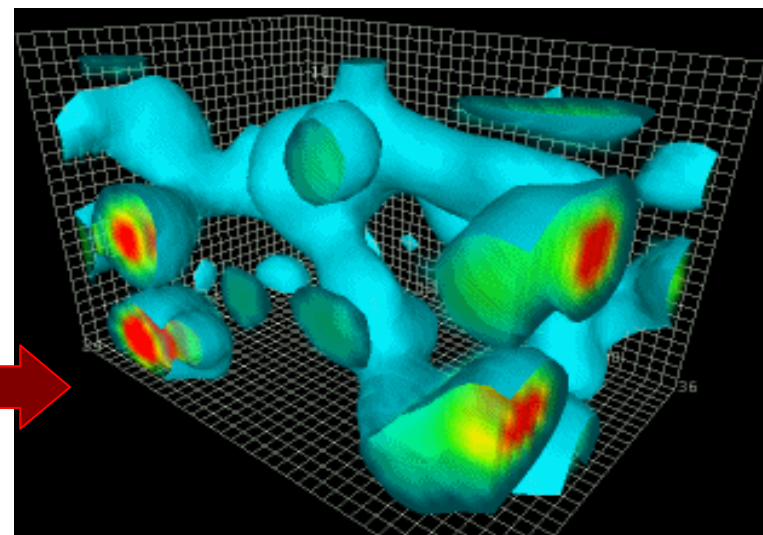
Color-flavor symmetry (locking) \leftrightarrow Diquark condensate at high density

QCD phase \leftrightarrow Symmetries of QCD \leftrightarrow QCD vacuum

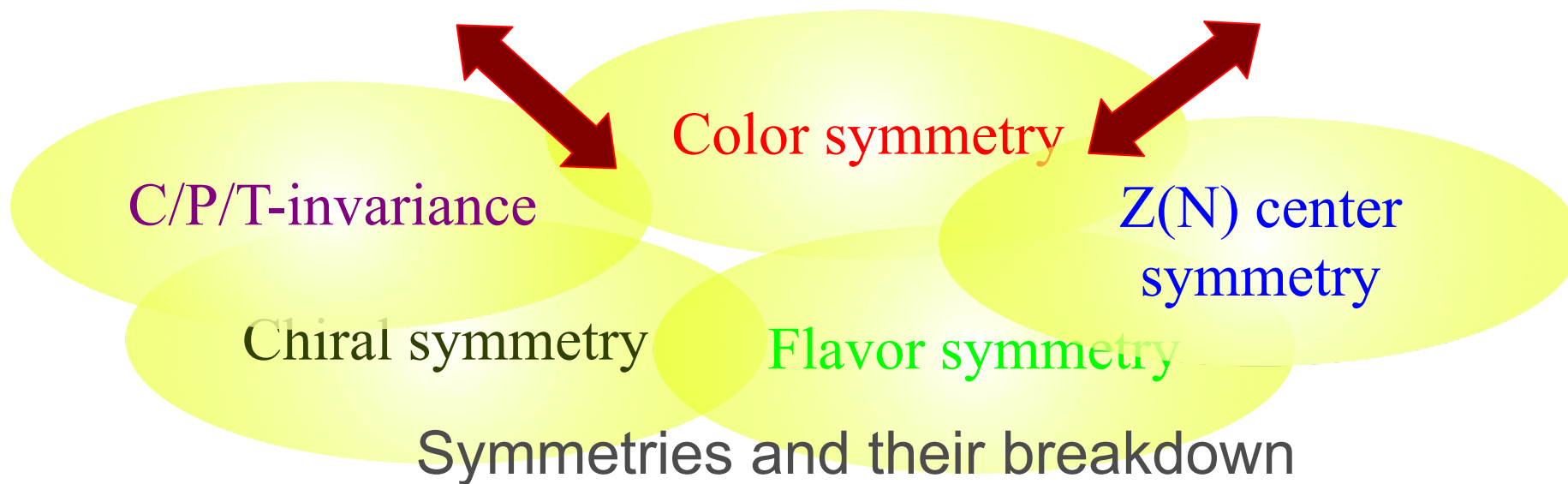
Why are heavy-ion collision experiments special for QCD?



Phase structure of QCD



Nontrivial QCD vacuum



2. QCD at extreme conditions

SCSB results in **nonzero** chiral (quark) condensate due to nonzero effective quark mass even in the chiral limit, i.e. $m=0$

$$-\langle \bar{\psi}\psi \rangle_{\text{Mink}} = i\langle \psi^\dagger\psi \rangle_{\text{Eucl}} = 4N_c \int \frac{d^4p}{(2\pi)^4} \frac{M(p)}{p^2 + M^2(p)}$$

Nonzero $\langle \underline{q}q \rangle$ indicates hadron (Nambu-Goldstone) phase, whereas zero $\langle \underline{q}q \rangle$ does non-hadronic phase, not meaning deconfinement

Thus, $\langle \underline{q}q \rangle$ is an order parameter for chiral symmetry

In the real world with nonzero quark current mass ~ 5 MeV, at low density, there appears crossover near $T \sim 0$, and it becomes 1st-order phase transition as density increases

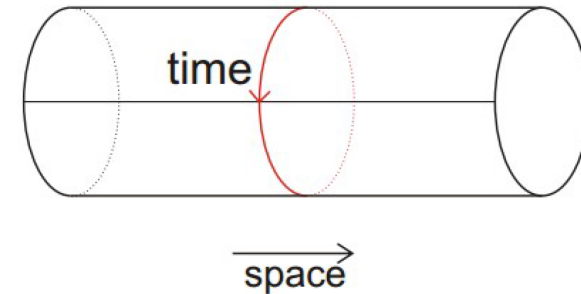
In the vicinity of critical density, there are various and complicated phases, such as color-superconducting, quarkyonic phase, etc.

2. QCD at extreme conditions

Dynamical (spontaneous) breakdown of center symmetry results in **nonzero Polyakov-loop condensate** $\langle L \rangle$

$$\begin{aligned}
 e^{-\beta F} &= \text{Tr}[e^{-H/T}] = \sum_n \langle n | e^{-\tau H} | n \rangle_{\tau=\beta=1/T} = \\
 &= \sum_n e^{-\beta E_n} = \\
 &= \sum_{\psi} \sum_U e^{-S_{FG}} \text{Tr} \psi_{\tau}^{\dagger} U_{\tau} U \dots U_0 \psi_0 = \\
 &= \sum_U e^{-S_G} \text{Tr}[UU \dots U]_{0\tau}
 \end{aligned}$$

$$\sum_U e^{-S_G} \underbrace{\text{Tr}[UU \dots U]_{0\tau}}_{\langle \text{Tr} P e^{ig \int_0^{\beta} A_0(\vec{x}) d\tau} \rangle_G} \rightarrow \langle L(\vec{x}) \rangle$$



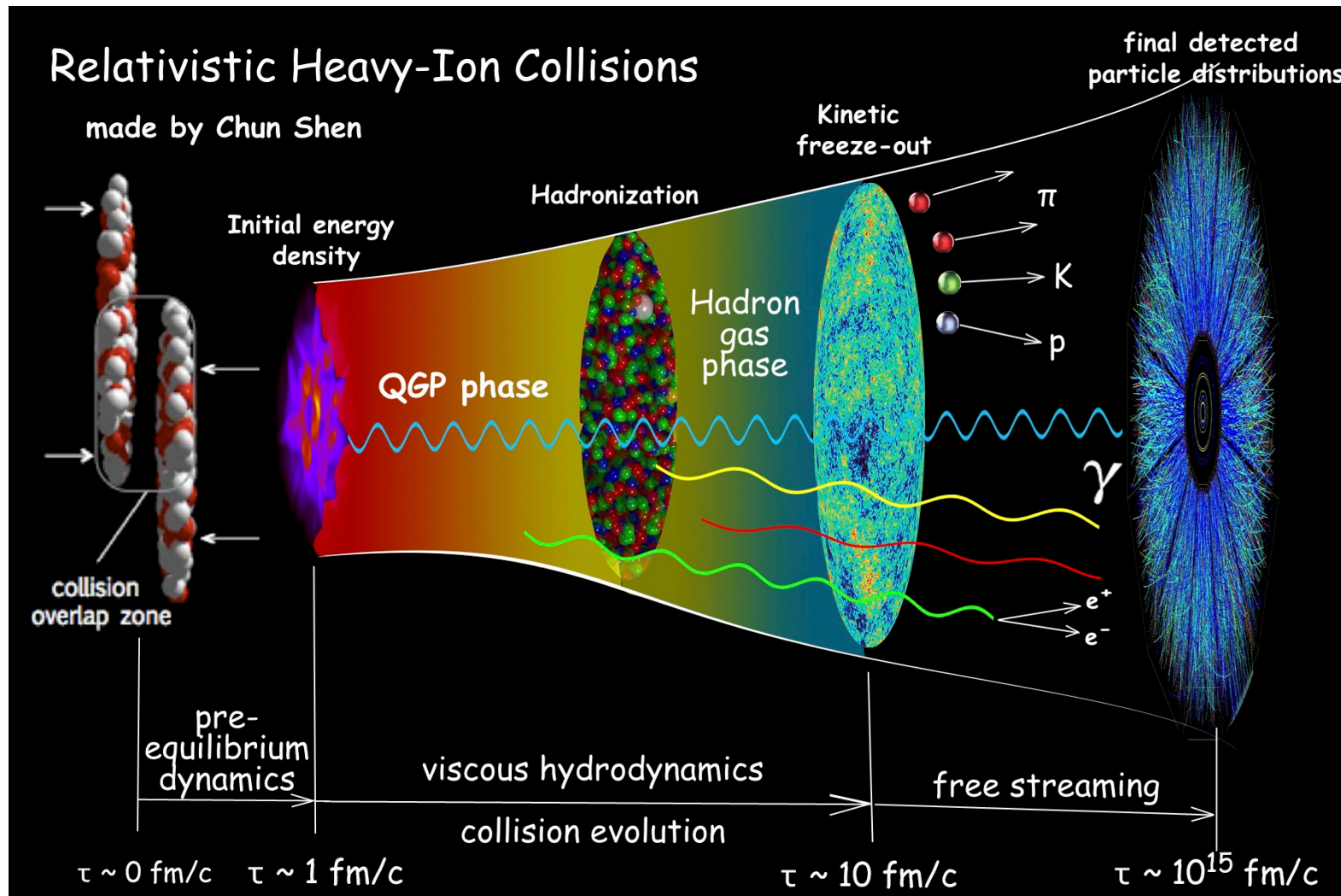
$$\begin{aligned}
 S_{0\tau} &= \psi_{\tau}^{\dagger} U_{\tau} U \dots U_0 \psi_0 : \\
 &\text{quark propagator } 0 \rightarrow \tau
 \end{aligned}$$

Considering $\text{Exp}[-F/T] \sim \langle L \rangle$, where F is quark free energy, “ $\langle L \rangle = 0$ ” means that F is infinity, so that quarks are confined

If $\langle L \rangle$ nonzero, F is finite to separate the quarks apart, i.e. deconfined

2. QCD at extreme conditions

Heavy-ion collision (HIC) experiments enable us to investigate hot and dense QCD matter ~ early Universe



2. QCD at extreme conditions

Theory can help to understand HIC experiments

Equation of state of QCD matter: Lattice QCD, Effective models

Evolution of QGP: (Viscous) Hydrodynamics

Hadronization: Transport models

We want to focus on the following subjects:

Critical behaviors, transport coefficients, Effects of external B fields...

For this purpose, we want to modify the effective models in terms of temperature (as well as density)

Polyakov-loop NJL model & T-modified LIM

3. Medium-modified Effective models

We start from the effective Lagrangian of NJL, resulting in effective thermodynamic potential Ω , which gives EoS of QCD matter

$$\mathcal{L} = \bar{\psi}(i\cancel{\partial} - \underline{m})\psi + G ((\bar{\psi}\psi)^2 + (\bar{\psi}i\gamma_5\tau_a\psi)^2)$$

We expand the four-quark interaction in terms of SBCS

$$\bar{\psi}\psi = \langle \bar{\psi}\psi \rangle_{NJL} + \delta(\bar{\psi}\psi)$$

Finite chiral condensate considered as an effective quark mass

$$M = m - 2G \langle \bar{\psi}\psi \rangle_{NJL}$$

Finally, we arrive at an effective Lagrangian manifesting SBCS

$$\mathcal{L} = \bar{\psi} (i\cancel{\partial} - M) \psi - \frac{(M - m)^2}{4G}$$

Free quark with effective mass M

Constant potential via SBCS

3. Medium-modified Effective models

Employing **Matsubara formula** to convert the action $S \sim \int d^4x$ Lagrangian into thermodynamic potential

$$i \int \frac{d^4k}{(2\pi)^4} f(k) \longrightarrow -T \sum_n \int \frac{d^3k}{(2\pi)^3} f(i\omega_n + \mu, \vec{k})$$

with fermionic Matsubara frequencies $\omega_n = (2n + 1)\pi T$

We arrive at an effective thermodynamic potential

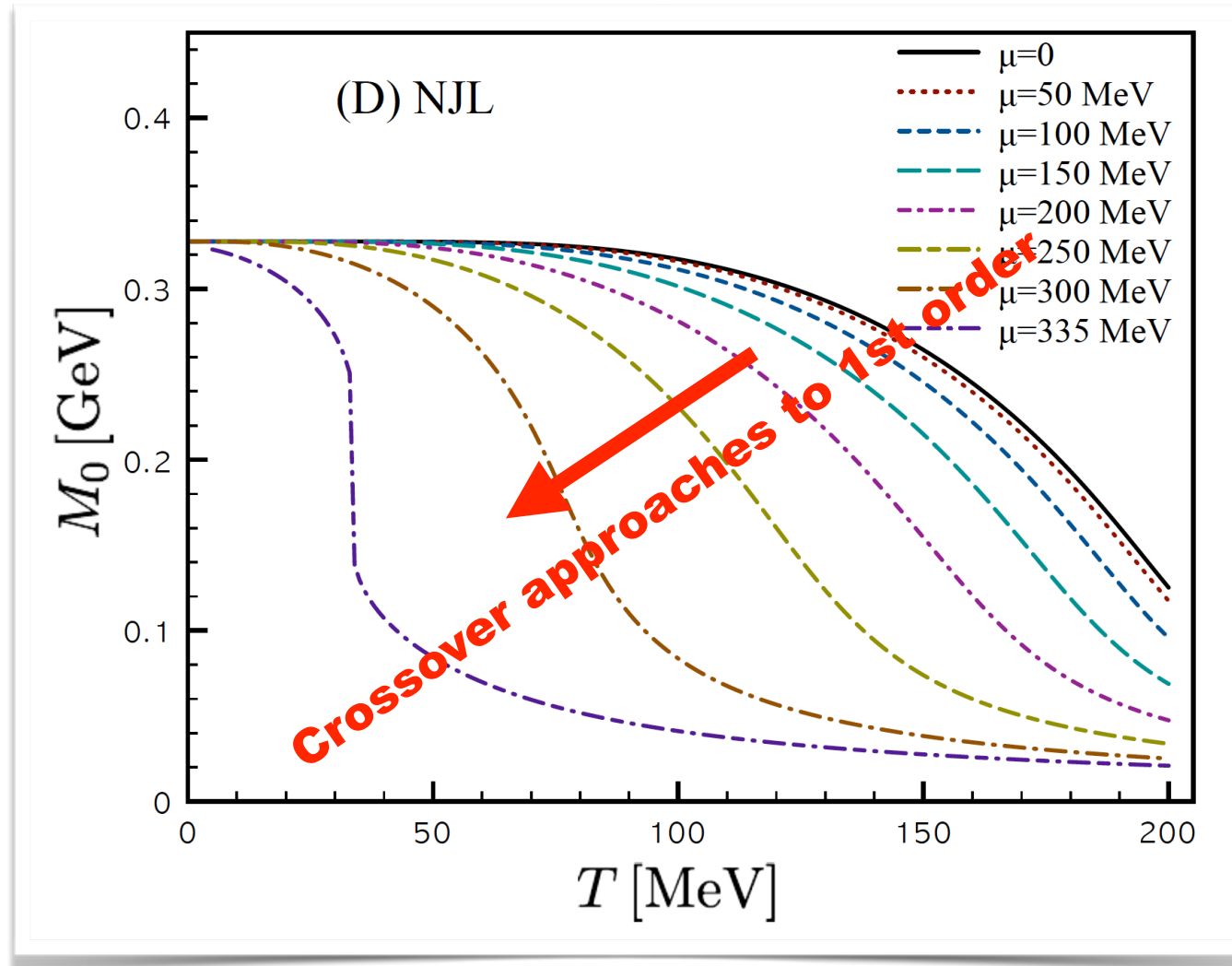
$$\Omega_{\text{NJL}} = \frac{(M_0 - m_q)^2}{4G} - 2N_c N_f \int_0^\Lambda \frac{d^3\mathbf{k}}{(2\pi)^3} \left\{ E_{\mathbf{k}0} + T \ln \left[\left(1 + e^{-\frac{E_{\mathbf{k}0} - \mu}{T}} \right) \left(1 + e^{-\frac{E_{\mathbf{k}0} + \mu}{T}} \right) \right] \right\}$$

Computing gap equation, giving phase diagram for SBCS

$$\frac{\partial \Omega_{\text{NJL}}}{\partial M_0} = \frac{M_0 - m_q}{2G} - 2N_c N_f \int_0^\Lambda \frac{d^3\mathbf{k}}{(2\pi)^3} \frac{M_0}{E_{\mathbf{k}0}} \left[1 - \frac{e^{-\frac{E_{\mathbf{k}0} - \mu}{T}}}{1 + e^{-\frac{E_{\mathbf{k}0} - \mu}{T}}} - \frac{e^{-\frac{E_{\mathbf{k}0} + \mu}{T}}}{1 + e^{-\frac{E_{\mathbf{k}0} + \mu}{T}}} \right] = 0$$

3. Medium-modified Effective models

QCD phase diagram as a function of T and μ via NJL model



3. Medium-modified Effective models

K. Fukushima develop a modified NJL with Polyakov loop, i.e **pNJL**

Identifying the imaginary quark chemical potential as Polyakov line,

$$\begin{aligned} \Omega/V = & V_{\text{glue}}[L] + \frac{1}{2G}(M - m_q)^2 \\ & - 2N_c N_f \int \frac{d^3 p}{(2\pi)^3} \left\{ E_p + T \frac{1}{N_c} \right. \\ & \times \text{Tr}_c \ln[1 + L e^{-(E_p - \mu)/T}] \\ & \left. + T \frac{1}{N_c} \text{Tr}_c \ln[1 + L^\dagger e^{-(E_p + \mu)/T}] \right\}, \end{aligned}$$

$$L(\vec{x}) = \mathcal{T} \exp \left[-i \int_0^\beta dx_4 A_4(x_4, \vec{x}) \right]$$

$$\begin{aligned} & V_{\text{glue}}[L] \cdot a^3 / T \\ & = -2(d-1)e^{-\sigma a/T} |\text{Tr}_c L|^2 \\ & \quad - \ln[-|\text{Tr}_c L|^4 + 8 \text{Re}(\text{Tr}_c L)^3 \\ & \quad - 18|\text{Tr}_c L|^2 + 27] \end{aligned}$$

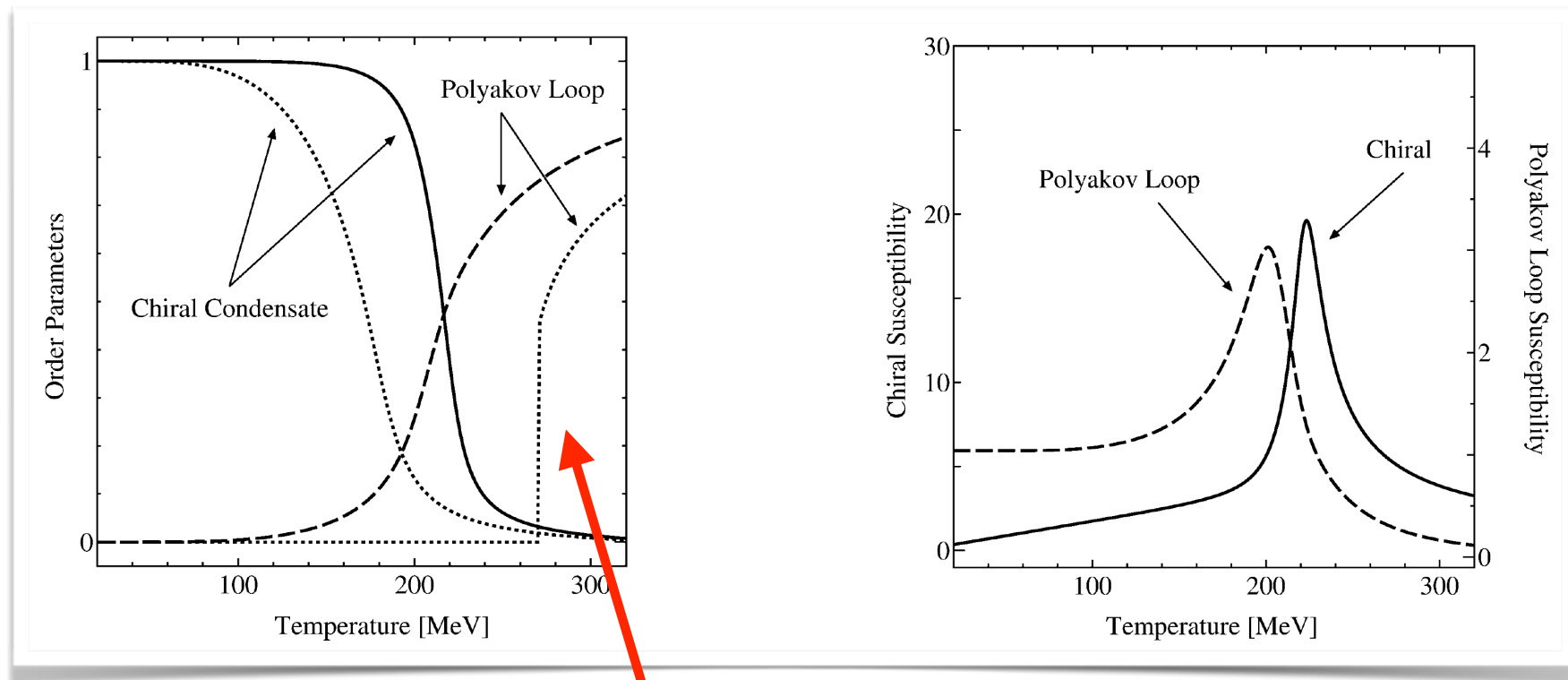
$V_{\text{glue}}[L]$ constructed by $Z(N_c)$ symmetry and lattice QCD information

$$\Omega_{\text{eff}}^\phi = -T^4 \left[\frac{b_2(T)}{2} (\phi \phi^*) + \frac{b_3}{6} (\phi^3 + \phi^{*3}) - \frac{b_4}{4} (\phi \phi^*)^2 \right]$$

$$b_2(T) = a_0 + a_1 \left[\frac{T_0}{T} \right] + a_2 \left[\frac{T_0}{T} \right]^2 + a_3 \left[\frac{T_0}{T} \right]^3$$

3. Medium-modified Effective models

Realization of simultaneous crossover of chiral and deconfinement phase transitions



Due to quark-L interaction, $\langle L \rangle$ shows crossover, rather than 1st order in pure-gluon theory

3. Medium-modified Effective models

T-modified LIM: (mLIM) Instanton parameters are modified with trivial-holonomy caloron solution (Not dyon, vortex, or something)

Caloron is an instanton solution for periodic in Euclidean time, i.e temperature, but no confinement

Distribution func. via trivial-holonomy (Harrington-Shepard) caloron

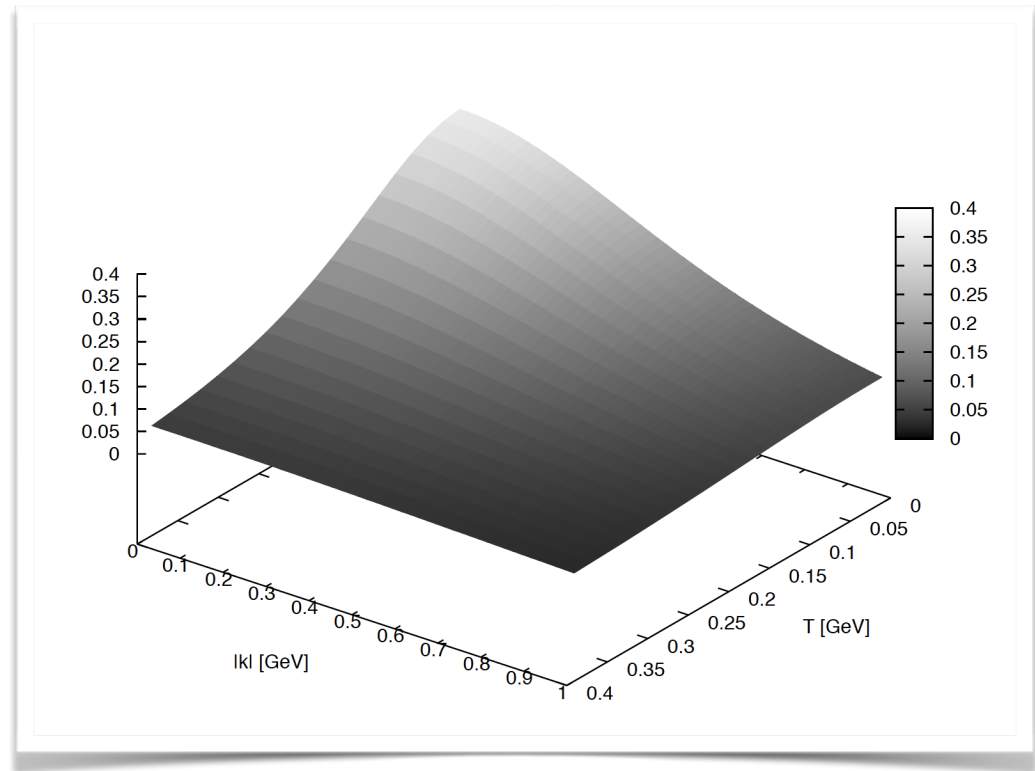
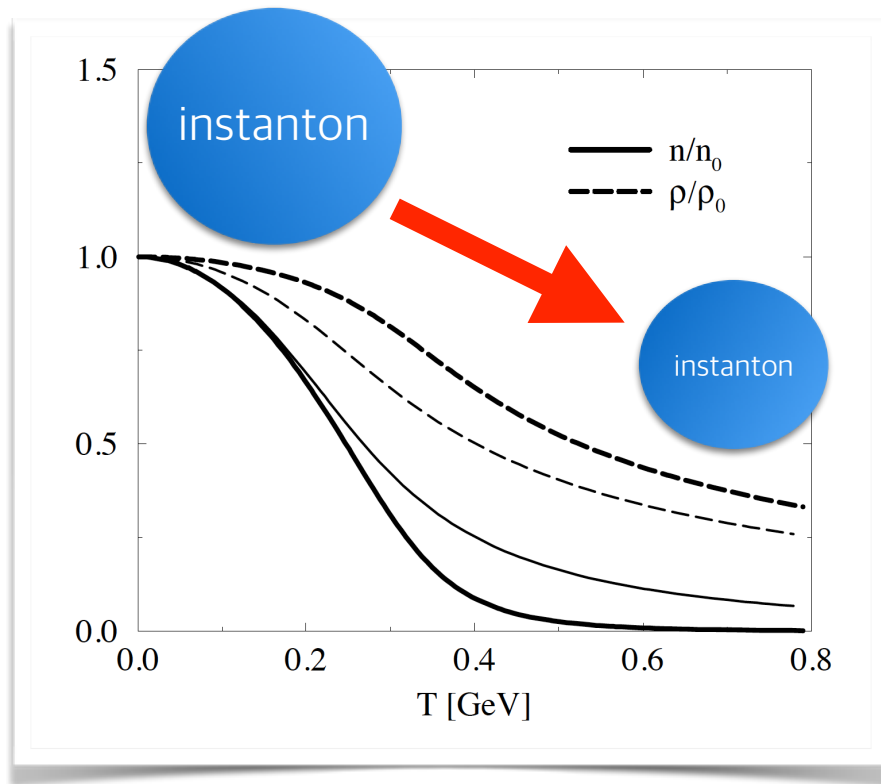
$$d(\rho, T) = C \rho^{b-5} \exp [-\mathcal{F}(T)\rho^2], \quad \mathcal{F}(T) = \frac{1}{2}A_{N_c}T^2 + \left[\frac{1}{4}A_{N_c}^2T^4 + \nu\bar{\beta}\gamma n \right]^{\frac{1}{2}}$$

$$A_{N_c} = \frac{1}{3} \left[\frac{11}{6}N_c - 1 \right] \pi^2, \quad \gamma = \frac{27}{4} \left[\frac{N_c}{N_c^2 - 1} \right] \pi^2, \quad b = \frac{11N_c - 2N_f}{3}$$

Using this, we modify the two instanton parameters as functions of T

3. Medium-modified Effective models

mLIM parameters (left) and effective quark mass M (right)

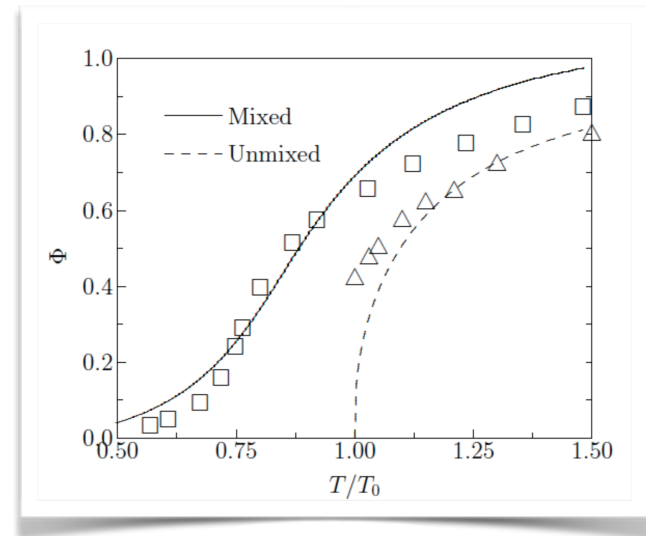


Hence, effective quark mass plays the role of UV regulator

3. Medium-modified Effective models

Finally, we arrive at an effective thermodynamic potential via instanton and Polyakov loop

$$\begin{aligned} \Omega_{\text{eff}} &= \Omega_{\text{eff}}^{\text{q}+\Phi} + \Omega_{\text{eff}}^{\Phi} = 2\sigma^2 - 2N_f \left[N_c \int \frac{d^3\mathbf{k}}{(2\pi)^3} E_{\mathbf{k},T} \right. \\ &+ T \int \frac{d^3\mathbf{k}}{(2\pi)^3} \ln \left[1 + N_c \left(\Phi + \bar{\Phi} e^{-\frac{E_{\mathbf{k},T}}{T}} \right) e^{-\frac{E_{\mathbf{k},T}}{T}} + e^{-\frac{3E_{\mathbf{k},T}}{T}} \right] \\ &+ T \int \frac{d^3\mathbf{k}}{(2\pi)^3} \ln \left[1 + N_c \left(\bar{\Phi} + \Phi e^{-\frac{E_{\mathbf{k},T}}{T}} \right) e^{-\frac{E_{\mathbf{k},T}}{T}} + e^{-\frac{3E_{\mathbf{k},T}}{T}} \right] \left. \right] \\ &- T^4 \left[\frac{b_2(T)}{2} (\Phi \bar{\Phi}) + \frac{b_3}{6} (\Phi^3 + \bar{\Phi}^3) - \frac{b_4}{4} (\Phi \bar{\Phi})^2 \right], \end{aligned}$$

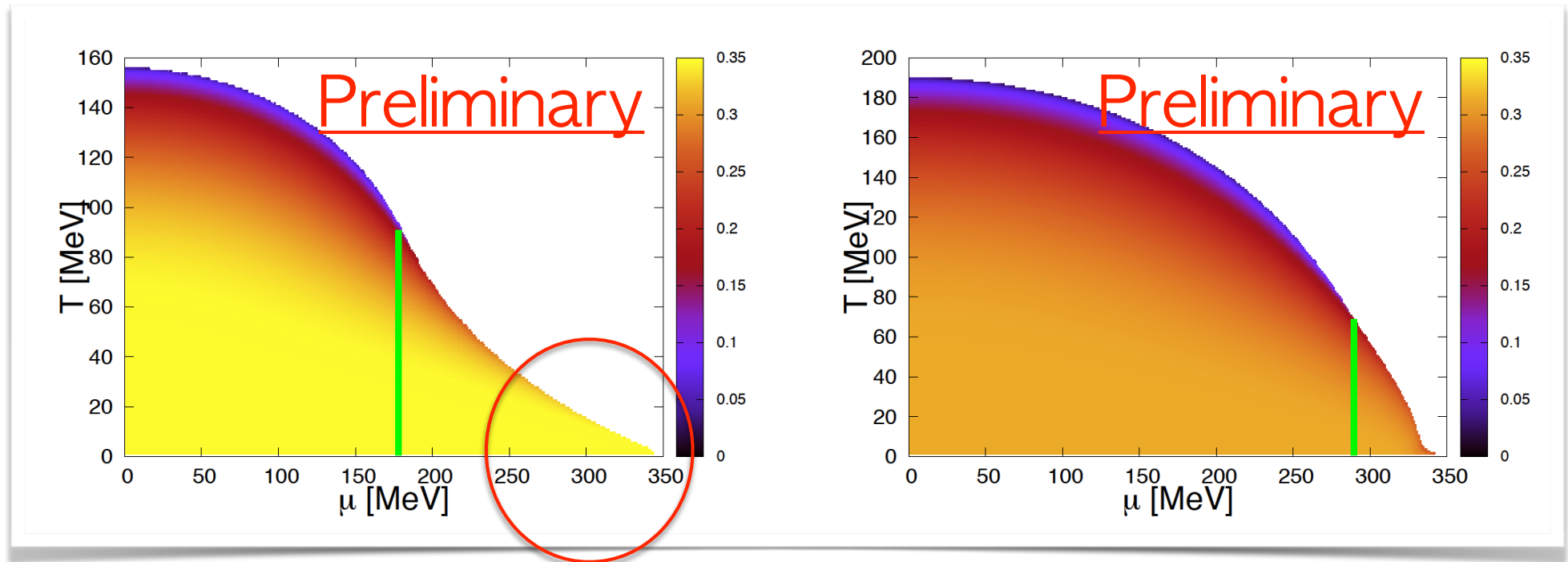


Basically, we have similar results with pNJL results

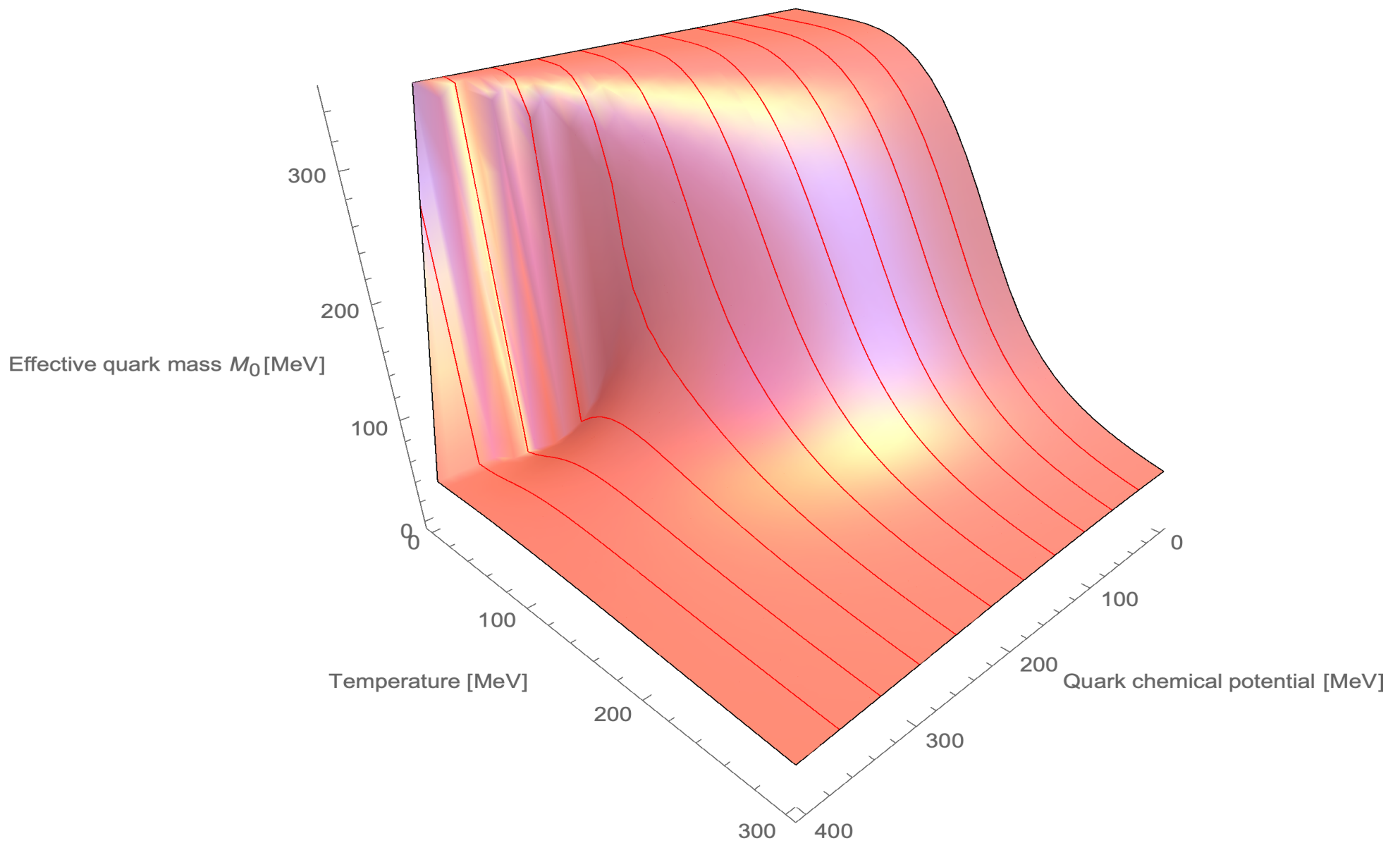
In detail, positions for critical T and ρ , structure of phase shift, etc. are different quantitatively

3. Medium-modified Effective models

We plot the phase diagrams via mLIM (left) and NJL (right)



The effects of T -dependent model parameters are obvious!



4. Some numerical results

Interesting subjects in hot and dense QCD (QGP) in terms of the strongly interacting quark-gluon matter

1. Phase structure: Where are CEP and TCP?
2. Effects of external magnetic fields: CME, CMS
3. Transport coefficients: Viscosities, conductivities, etc.
4. Contributions from flavors, colors, axial anomaly
5. Various current-current correlators: Jet-quenching parameter
6. LEC in color fields
- 7...

Very rapidly developing fields

Much relations with lattice QCD community

Still huge amounts of research subjects waiting for you!



WE NEED YOU!

4. Some numerical results

This time, I focus on

Transport coefficients under external magnetic fields

QGP and Transport coefficients:

Recent heavy-ion collision experiment showed possible evidence of QGP

Interpreted well by hydrodynamics with small viscosity \sim perfect fluid

Properties of QGP can be understood by transport coefficients:
Bulk and shear viscosities, electrical conductivity, and so on

They can be studied using **Kubo formula** via linear response theory

Introduction

QGP and transport coefficients

- Recent heavy-ion collision experiment showed possible evidence of QGP
- Interpreted well by hydrodynamics with small viscosity: \sim perfect fluid
J. Adams et al. [STAR Collaboration], Nucl. Phys. A, 102 (2005)
- Properties of QGP can be understood by transport coefficients:

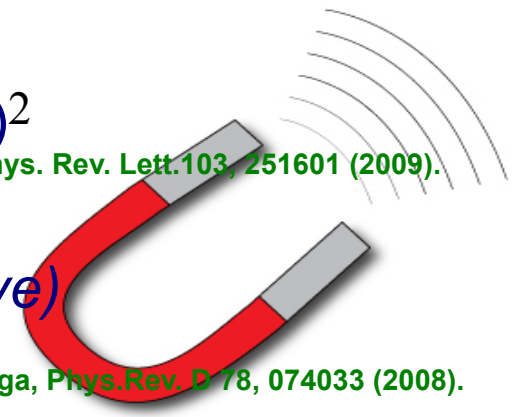
Bulk and shear viscosities, electrical conductivity, and so on

- They can be studied using Kubo formulae via linear response theory

F. Karsch, D. Kharzeev, and K. Tuchin, Phys. Lett. B 663, 217 (2008).

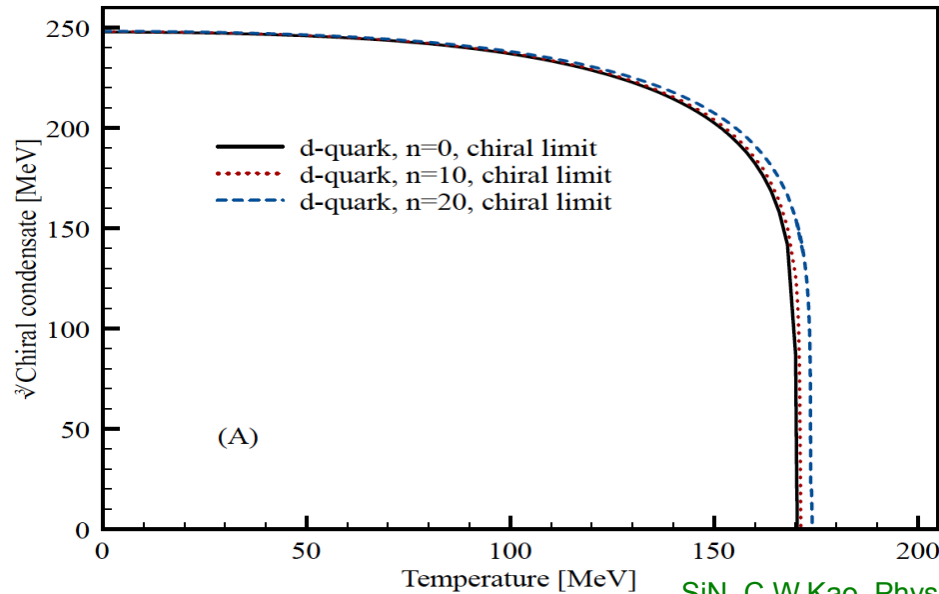
Strong magnetic (B) field in QGP

- RHIC experiments observed strong B field \sim (pion mass)²
B. I. Abelev et al. (STAR Collaboration), Phys. Rev. Lett. 103, 251601 (2009).
- Strong B field modify nontrivial QCD vacuum structure
- Charged-current asymmetry: *Chiral magnetic effect (wave)*
- B field enhances SBCS: *Magnetic catalysis*
K. Fukushima, D. E. Kharzeev, and H. J. Warringa, Phys. Rev. D 78, 074033 (2008).

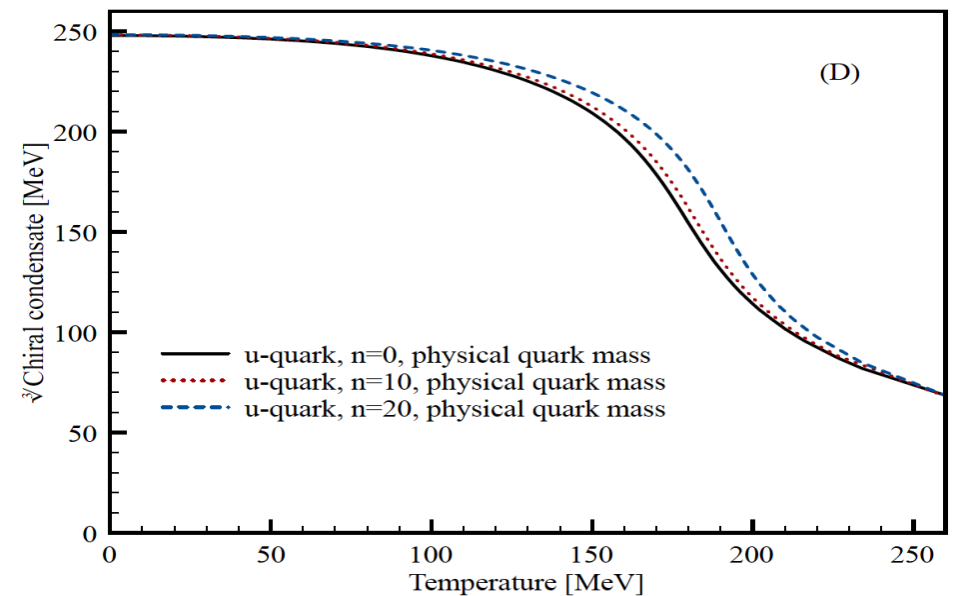
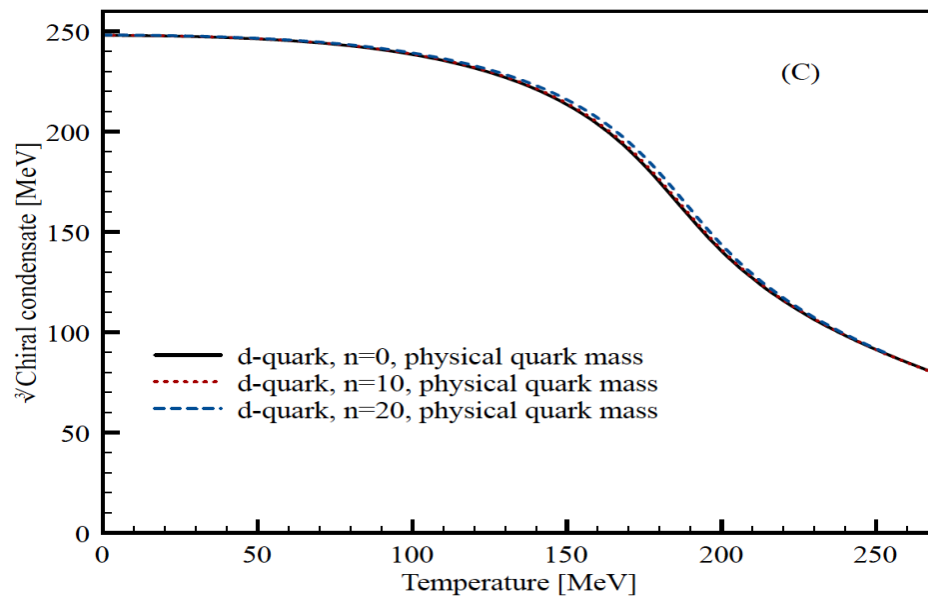
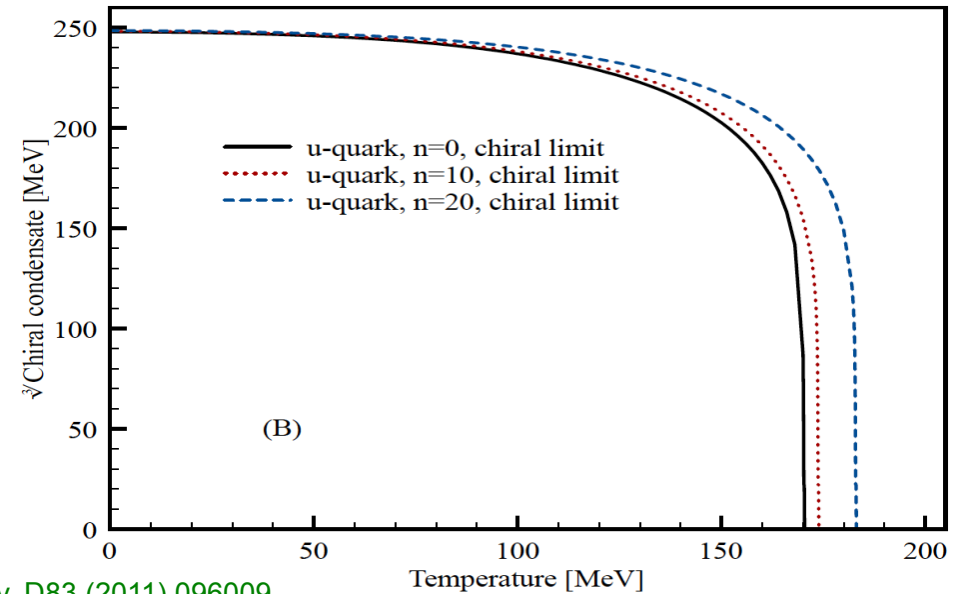


D. P. Menezes, M. Benghi Pinto, S. S. Avancini, A. Perez Martinez, and C. Providencia, Phys. Rev. C 79, 035807 (2009).

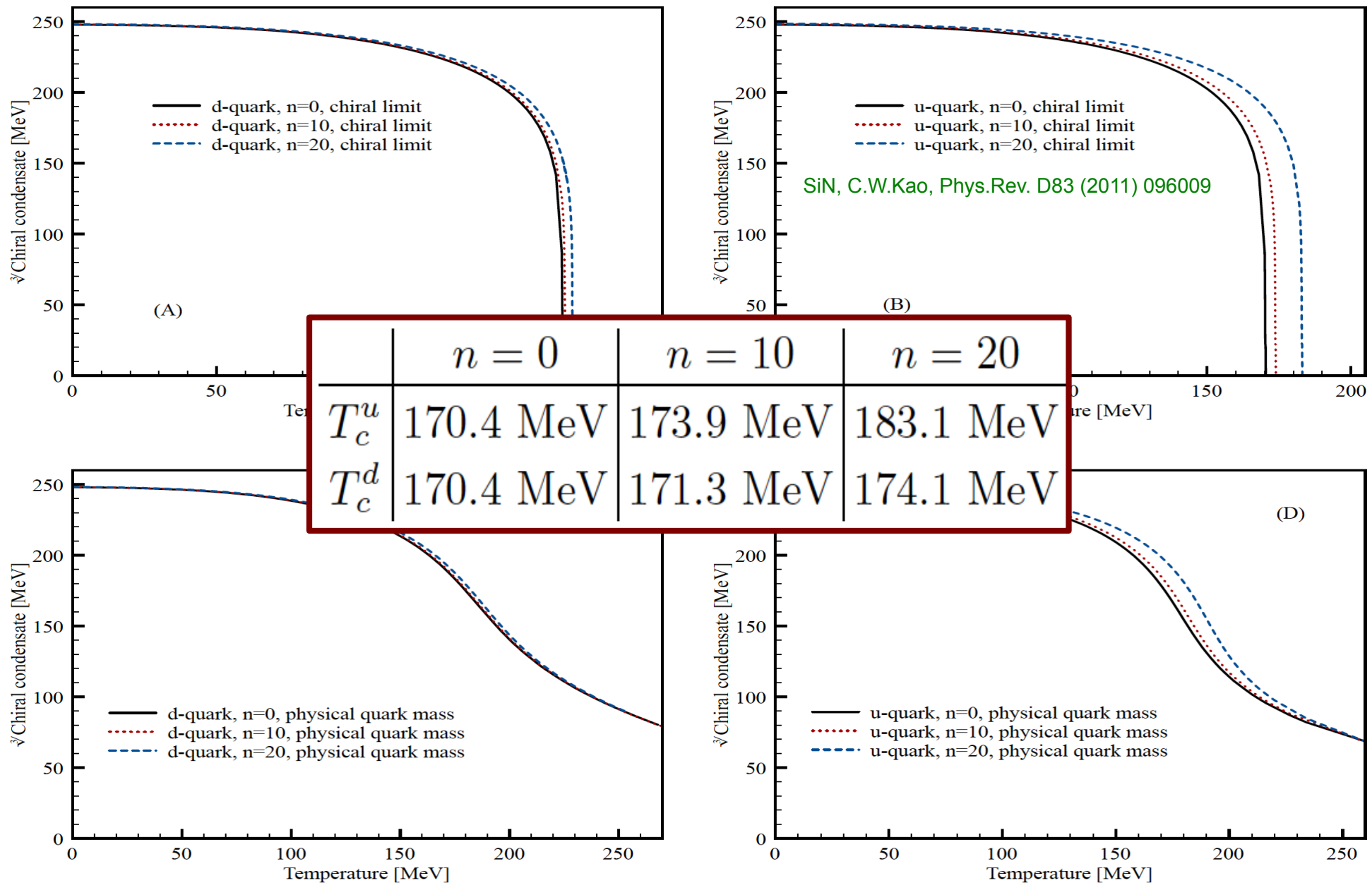
Chiral condensate for u and d flavors under B field



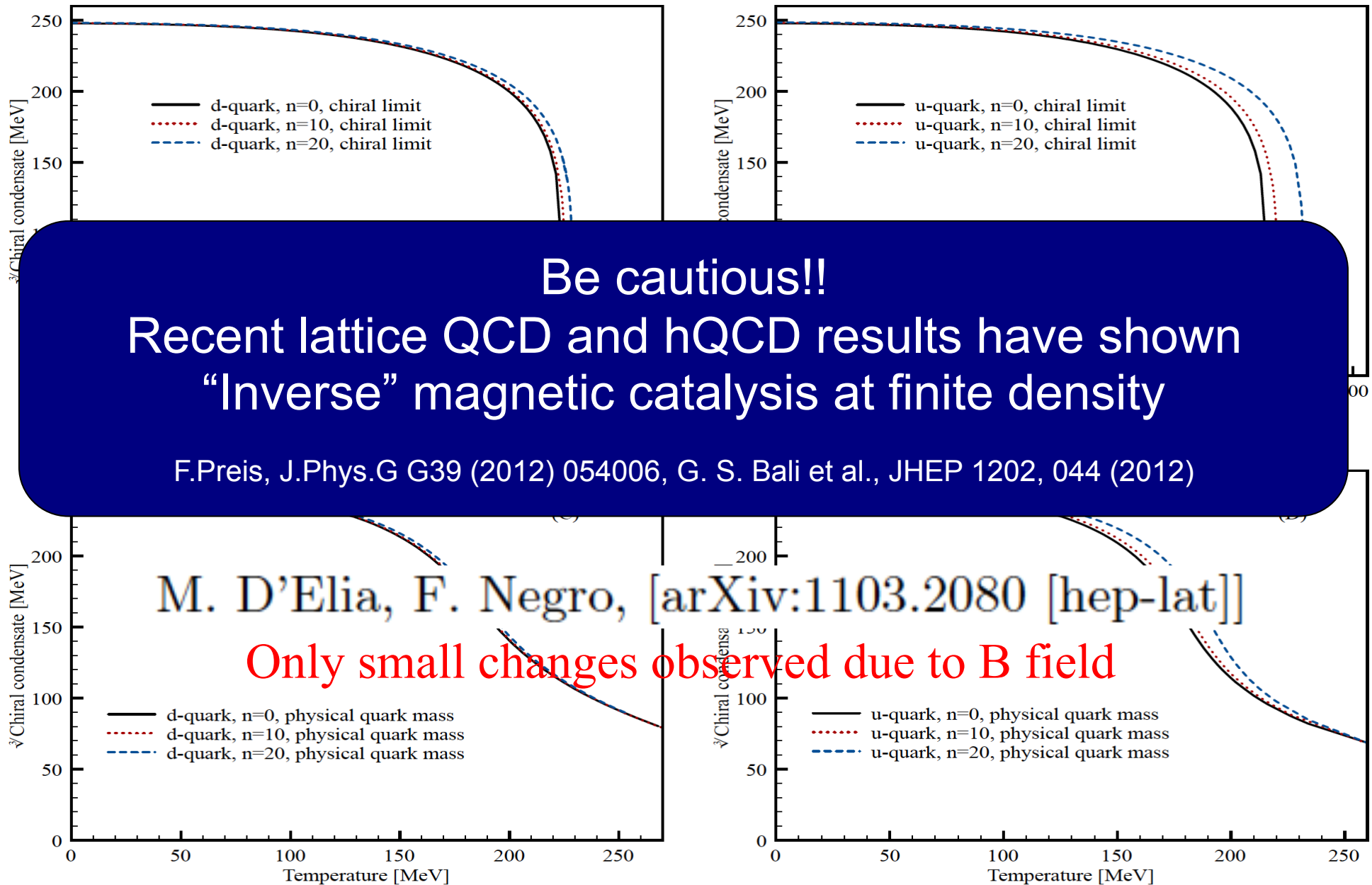
SiN, C.W.Kao, Phys.Rev. D83 (2011) 096009



Chiral condensate for u and d flavors under B field



Chiral condensate for u and d flavors under B field

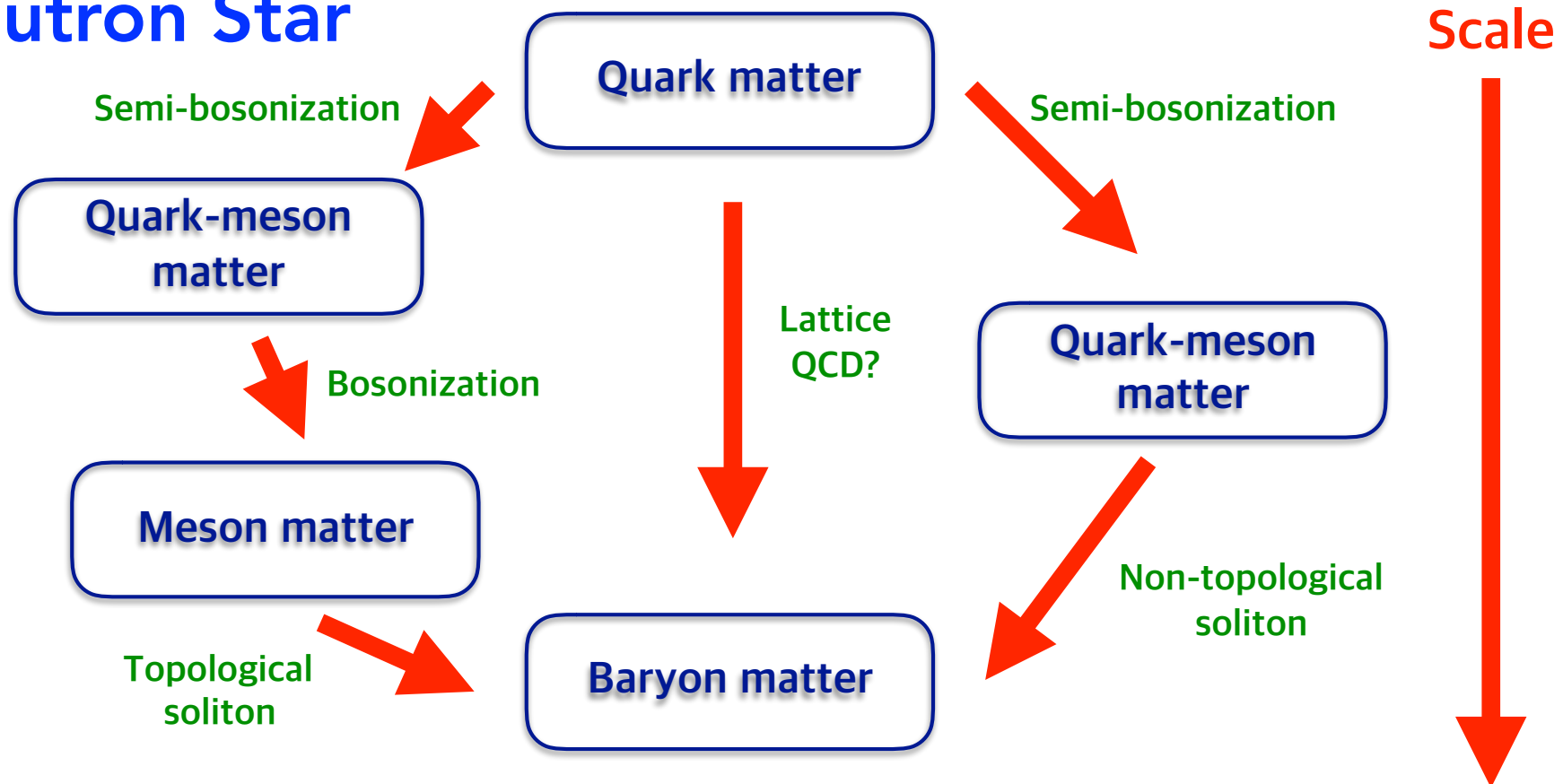


Medium-modified Effective model: EoS

Thermodynamic properties of matter can be understood by EoS

Neutron star in terms of effective Dofs: Smooth transition possible?

Neutron Star



Medium-modified Effective model in SU(2_f)

Effective action from liquid-instanton vacuum (Euclidean)

$$\mathcal{S}_{\text{eff}} = -\frac{N}{V} \ln \left[\frac{N}{V} \frac{2\pi^2 \bar{\rho}^2}{N_c M_0 M} \right] - 2N_c \int \frac{d^4 k}{(2\pi)^4} \ln \left[\frac{k^2 + \bar{M}_k^2}{k^2 + m^2} \right]$$

Matsubara frequency for fermions

$$\int \frac{d^4 k}{(2\pi)^4} f[k_4, \mathbf{k}] \rightarrow T \sum_{n=-\infty}^{\infty} \int \frac{d^3 \mathbf{k}}{(2\pi)^3} f[(2n+1)\pi T, \mathbf{k}]$$

Thermodynamic potential from LIM and NJL

$$\Omega_{\text{eff}}^{\text{LIM}} = \Omega_{\text{eff}}^g + \Omega_{\text{eff}}^q = -\frac{N_f N}{V} \ln \left[\frac{N}{V} \frac{2\pi^2 \bar{\rho}^2}{N_c M_0 M} \right] - 2N_c N_f \int \frac{d^3 \mathbf{k}}{(2\pi)^3} [E + T \ln [(1+Y)(1+X)]],$$

$$\Omega_{\text{eff}}^{\text{NJL}} = \frac{(\mathcal{M} - m)^2}{4G} - 2N_c N_f \int^{\Lambda} \frac{d^3 \mathbf{k}}{(2\pi)^3} [\mathcal{E} + T \ln [(1+\mathcal{Y})(1+\mathcal{X})]].$$

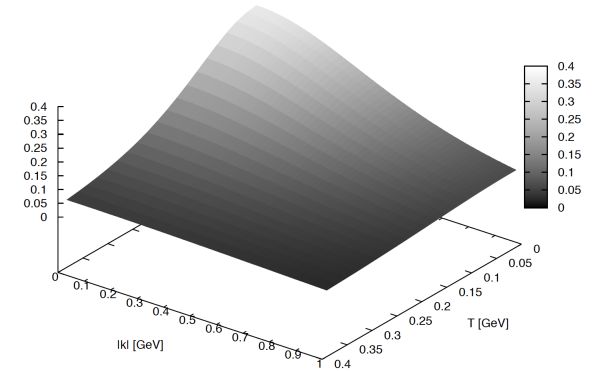
$$X = e^{-E_+/T}, \quad Y = e^{-E_-/T}, \quad E_{\pm} \equiv E \pm \mu = \sqrt{\mathbf{k}^2 + (m + M^2)} \pm \mu,$$

$$\mathcal{X} = e^{-\mathcal{E}_+/T}, \quad \mathcal{Y} = e^{-\mathcal{E}_-/T}, \quad \mathcal{E}_{\pm} \equiv \mathcal{E} \pm \mu = \sqrt{\mathbf{k}^2 + (m + \mathcal{M})^2} \pm \mu.$$

Medium-modified Effective model

Momentum-dependent effective quark mass

$$M = M_0(\mu, T) \left[\frac{2}{2 + \bar{\rho}^2 \mathbf{k}^2} \right]^{\mathcal{N}}$$



Gap (saddle-point) equations for LIM and NJL

$$\frac{NN_f}{VM_0} = 2N_c N_f \int \frac{d^3\mathbf{k}}{(2\pi)^3} \frac{(m+M)F^{\mathcal{N}}}{E} \left[\frac{(1-XY)}{(1+X)(1+Y)} \right],$$

$$\frac{\mathcal{M}-m}{2G} = 2N_c N_f \int^{\Lambda} \frac{d^3\mathbf{k}}{(2\pi)^3} \frac{(m+\mathcal{M})}{\mathcal{E}} \left[\frac{1-\mathcal{X}\mathcal{Y}}{(1+\mathcal{X})(1+\mathcal{Y})} \right],$$

Parameterization of instanton packing fraction in medium

$$\frac{N}{V} \rightarrow \frac{N}{V} \left[\frac{M_0}{M_{0,\text{vac.}}} \right]^2$$

Medium-modified Effective model

Standard representations for thermodynamic properties of QCD matter

$$p(T, \mu) = -(\Omega - \Omega_{\text{vac.}}), \quad n(T, \mu) = -\frac{\partial \Omega}{\partial \mu},$$

$$s(T, \mu) = -\frac{\partial \Omega}{\partial T}, \quad \epsilon(T, \mu) = T s(T, \mu) + \mu n(T, \mu) - p(T, \mu),$$

Thermodynamic properties of QCD matter for LIM and NJL

$$p_{\text{NJL}} = -(\Omega_{\text{eff}}^{\text{NJL}} - \Omega_{\text{eff,vac.}}^{\text{NJL}}),$$

$$n_{\text{NJL}} = 2N_f N_c \int \frac{d^3 \mathbf{k}}{(2\pi)^3} \left[\frac{\mathcal{E}(\mathcal{Y} - \mathcal{X}) + (1 - \mathcal{X}\mathcal{Y})\mathcal{M}\mathcal{M}^{(\mu)}}{\mathcal{E}(1 + \mathcal{X})(1 + \mathcal{Y})} \right] - \frac{(\mathcal{M} - m)\mathcal{M}^{(\mu)}}{2G},$$

$$s_{\text{NJL}} = 2N_f N_c \int \frac{d^3 \mathbf{k}}{(2\pi)^3} \left[\ln [(1 + \mathcal{X})(1 + \mathcal{Y})] + \frac{\mathcal{E}[\mathcal{E}_-(1 + \mathcal{X})\mathcal{Y} + \mathcal{E}_+(1 + \mathcal{Y})\mathcal{X}] + T(1 - \mathcal{X}\mathcal{Y})\mathcal{M}\mathcal{M}^{(T)}}{\mathcal{E}T(1 + \mathcal{X})(1 + \mathcal{Y})} \right]$$

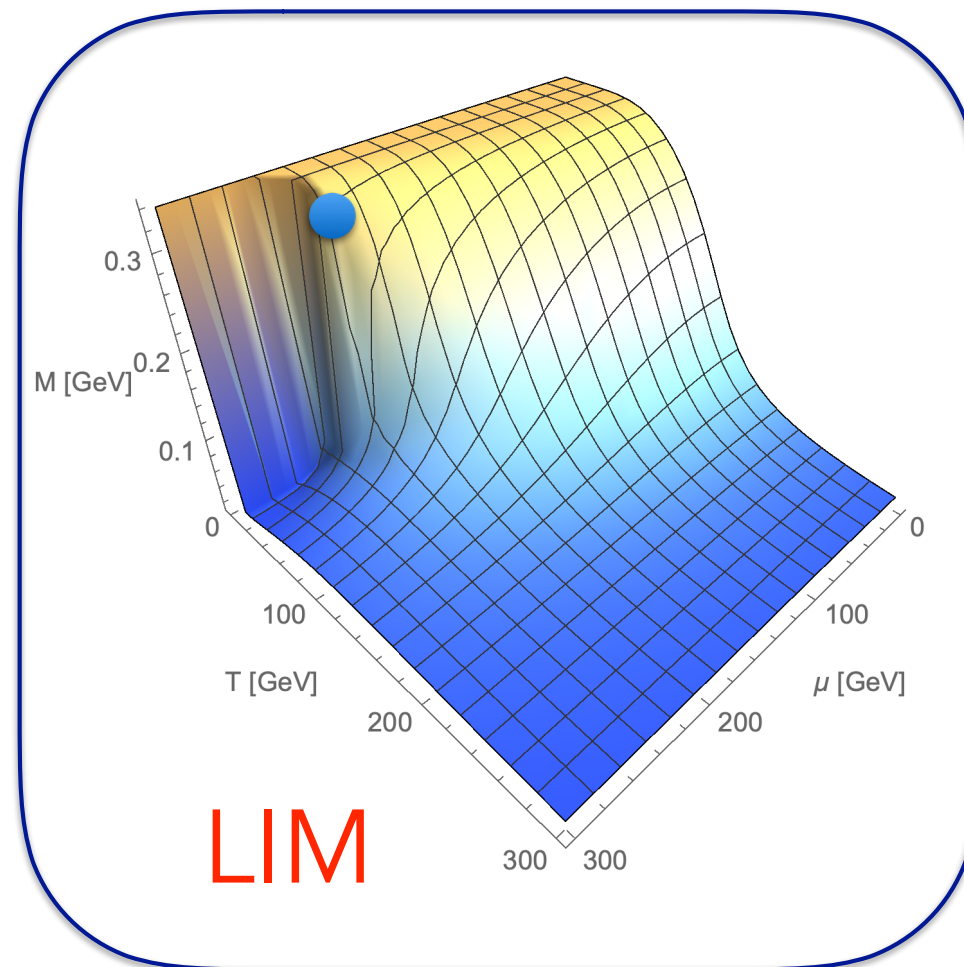
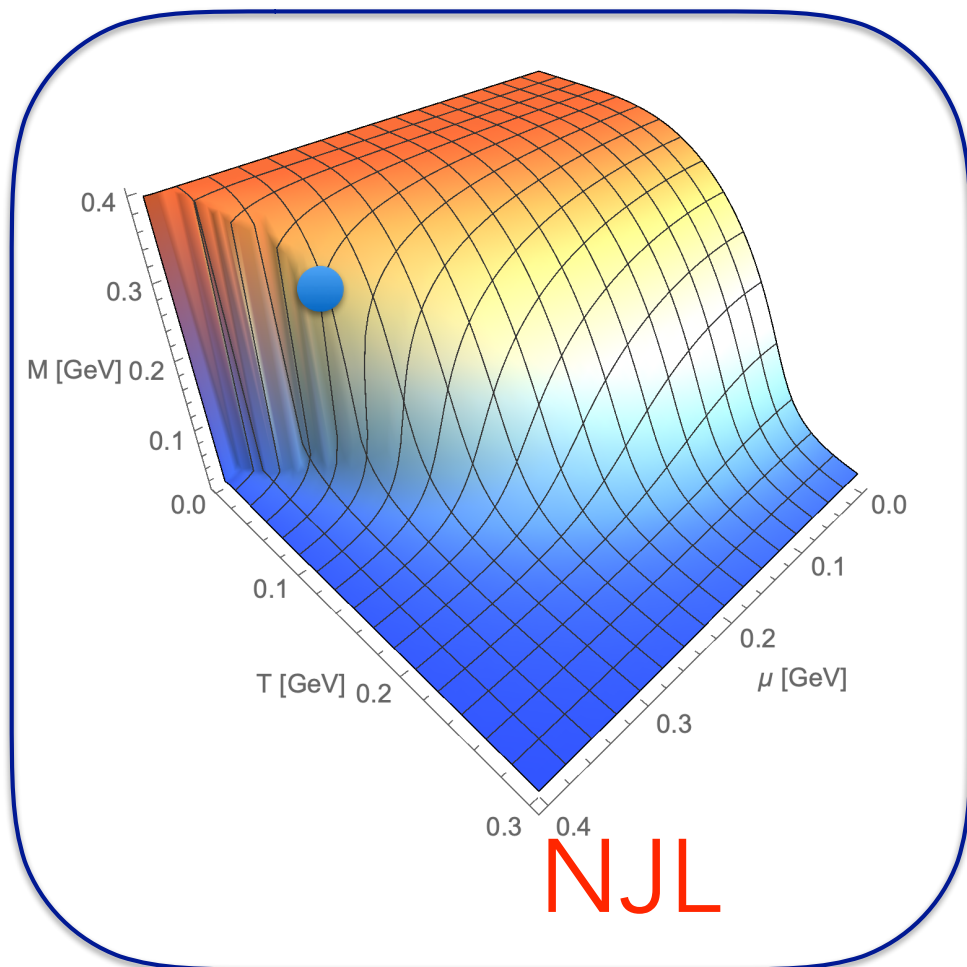
$$- \frac{(\mathcal{M} - m)\mathcal{M}^{(T)}}{2G}.$$

$$p_{\text{LIM}} = -(\Omega_{\text{eff}}^{\text{LIM}} - \Omega_{\text{eff,vac.}}^{\text{LIM}}),$$

$$n_{\text{LIM}} = 2N_f N_c \int \frac{d^3 \mathbf{k}}{(2\pi)^3} \left[\frac{E(Y - X) + (1 - XY)MM^\mu}{E(1 + X)(1 + Y)} \right] - \frac{2M_0 M_0^\mu N}{M_{0,\text{vac.}}^2 V}$$

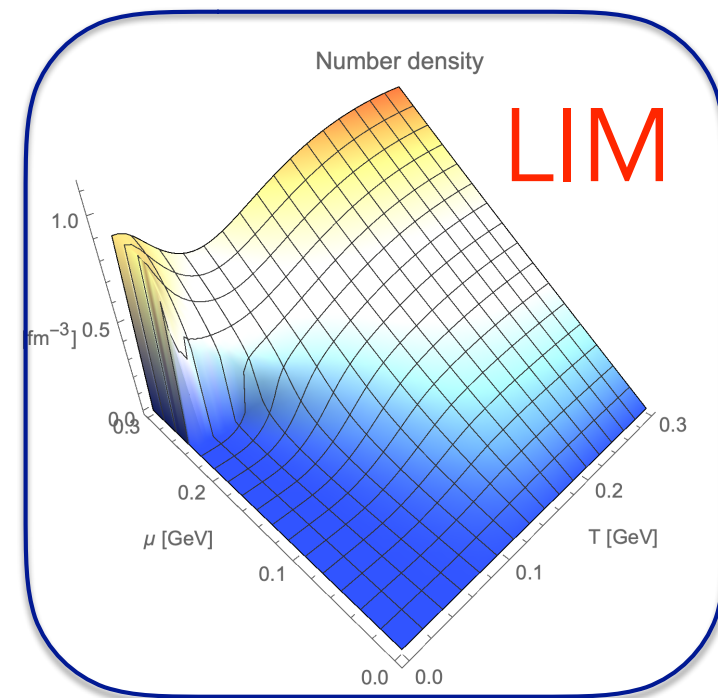
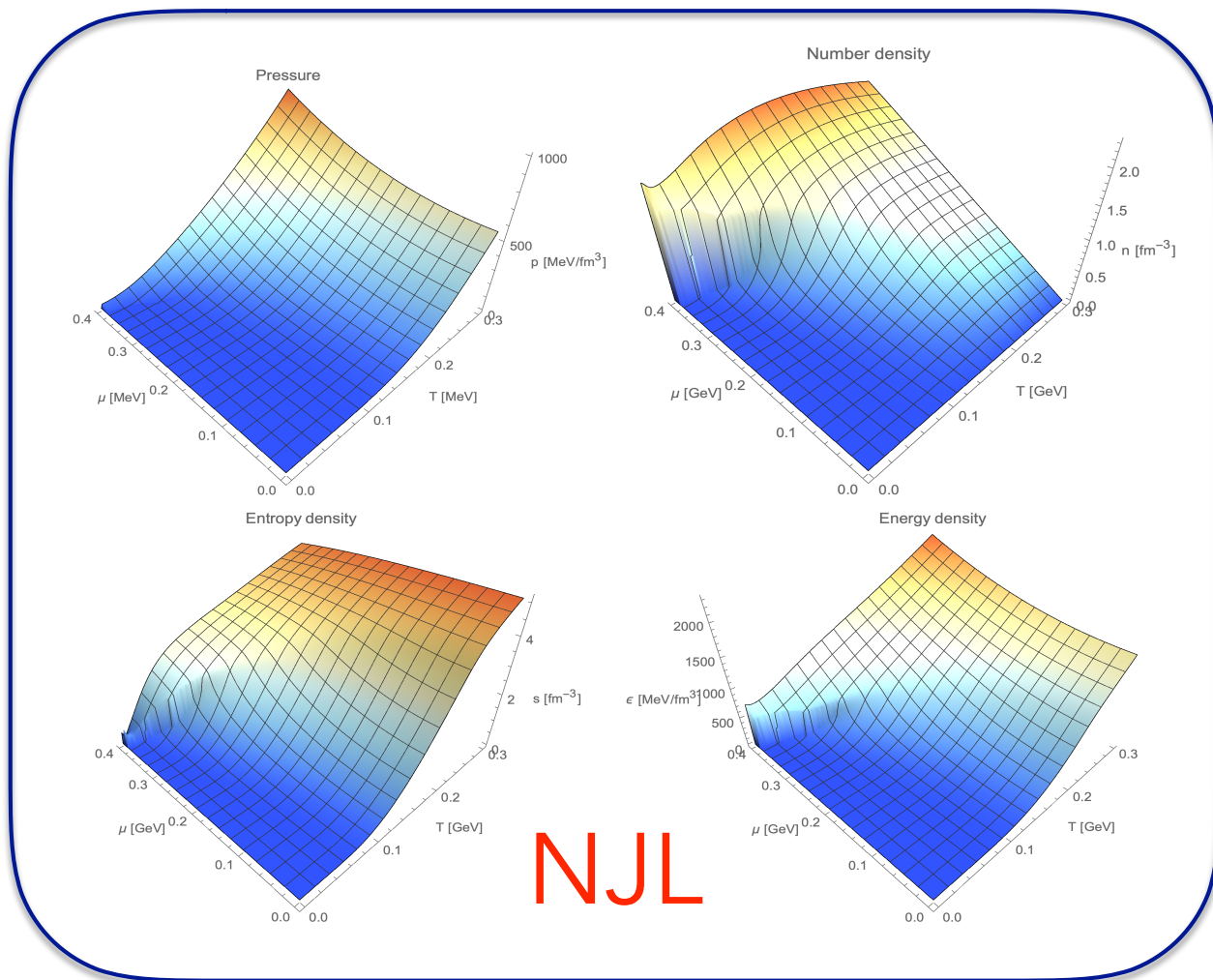
$$s_{\text{LIM}} = 2N_f N_c \int \frac{d^3 \mathbf{k}}{(2\pi)^3} \left[\ln [(1 + X)(1 + Y)] + \frac{E[E_-(1 + X)Y + E_+(1 + Y)X] + T(1 - XY)MM^{(T)}}{ET(1 + X)(1 + Y)} \right] - \frac{2M_0 M_0^{(T)} N}{M_{0,\text{vac.}}^2 V}$$

Thermodynamic properties: NJL vs. LIM



Chiral phase diagram via effective quark mass

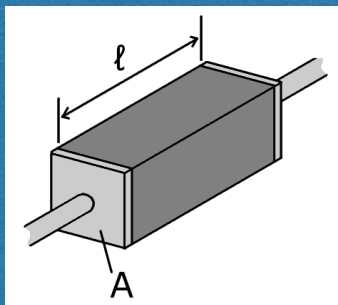
Thermodynamic properties: NJL vs. LIM



4. Some numerical results

Various transport coefficients

Electric conductivity

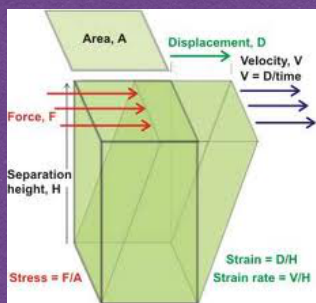


Heat conductivity

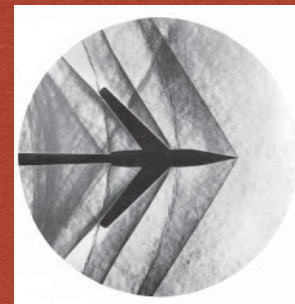


**Kubo formula:
Current-current
correlation**

Shear viscosity



Bulk viscosity



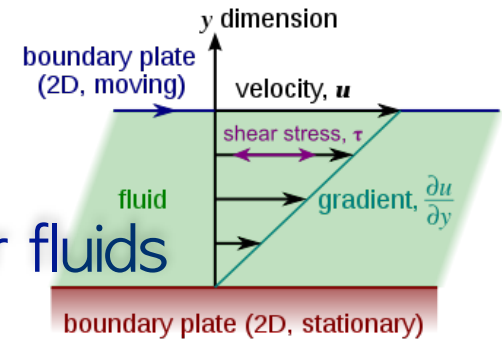
4. Some numerical results

Shear viscosity (η)

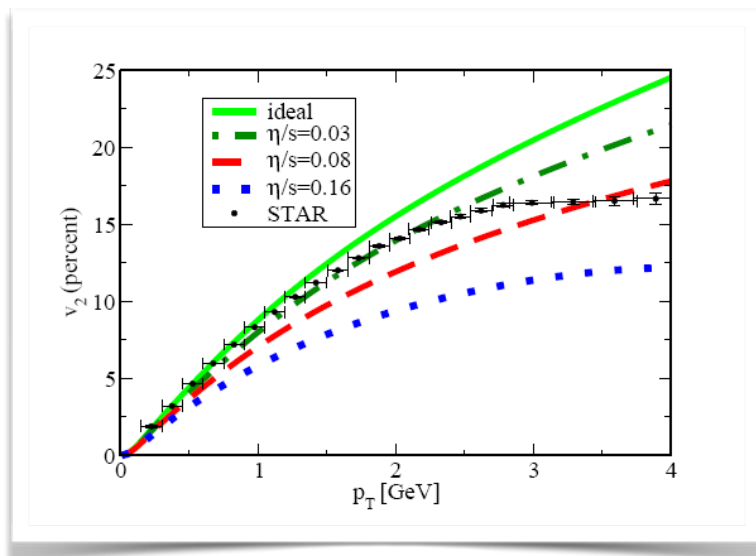
η amounts strength of the shear force for fluids

$$\frac{F}{A} = \eta \frac{u}{y}$$

Small shear viscosity means “not sticky”



In viscous hydrodynamics simulations, η of QGP used as a parameter



Small η \rightarrow



Large η \rightarrow



4. Some numerical results

η can be written in terms of the following **Kubo formula**

$$\eta = -\frac{\partial}{\partial \omega} \text{Im}[\Pi_{\text{R}}^{\eta}(\omega)]|_{\omega=+0}$$

The retarded Green function is obtained by

$$\Pi_{\text{R}}^{\eta}(\omega) = \Pi_{\text{M}}^{\eta}(i\omega)|_{i\omega \rightarrow \omega+i\epsilon}$$

The correlation for shear viscosity in Minkowski space reads

$$\Pi_{\text{M}}^{\eta}(i\omega) = -\int_0^{1/T} d\tau e^{-i\omega\tau} \int d\mathbf{r} \langle 0 | \mathcal{T} [J_{xy}(\mathbf{r}, \tau), J_{xy}(0, 0)] | 0 \rangle, \quad J_{xy} = \frac{i}{2} [\bar{\psi}(\gamma_y \partial_x \psi) - (\partial_x \bar{\psi}) \gamma_y \psi]$$

Rewriting the Matsubara sum into residue integral, we have

$$\begin{aligned} \Pi_{\text{M}}^{\eta}(i\omega) &= T \int \frac{d^3 \mathbf{k}}{(2\pi)^3} \sum_{n=-\infty}^{\infty} \text{Tr}_{c,f,\gamma} [k_x \gamma_y S(i\omega + i\omega_n, \mathbf{k}) k_x \gamma_y S(i\omega_n, \mathbf{k})] \\ &= -\oint \frac{dz}{2\pi i} \int \frac{d^3 \mathbf{k}}{(2\pi)^3} n_F(z) \text{Tr}_{c,f,\gamma} [k_x \gamma_2 S(i\omega + z, \mathbf{k}) k_x \gamma_2 S(z, \mathbf{k})] \end{aligned}$$

4. Some numerical results

We have the analytic expression with the quark spectral function

$$\begin{aligned}\eta &= -\frac{N_c N_f}{2} \lim_{\omega \rightarrow +0} \int \frac{dk_0}{2\pi} \frac{d^3 \mathbf{k}}{(2\pi)^3} \frac{[n_F(k_0 + \omega) - n_F(k_0)]}{\omega} k_x^2 \text{Tr}_\gamma [\rho(k_0 + \omega) \gamma_2 \rho(k_0) \gamma_2] \\ &= -\frac{N_c N_f}{2} \int \frac{dk_0}{2\pi} \frac{d^3 \mathbf{k}}{(2\pi)^3} n'_F(k_0) k_x^2 \text{Tr}_\gamma [\rho(k_0, \mathbf{k}) \gamma_2 \rho(k_0, \mathbf{k}) \gamma_2].\end{aligned}$$

Here, we used $n'_F = \frac{\partial n_F(z)}{\partial z}$ and $S(k_0, \mathbf{k}) = \int_{-\infty}^{\infty} \frac{dw}{2\pi} \frac{\rho(w, \mathbf{k})}{k_0 - w}$

Warning!! if the quark spectral function is a delta-function type, then shear viscosity becomes zero: To go beyond mean-field level

We consider finite-width quark spectral function

$$\rho_{\text{FW}}(w, \mathbf{k}) = 2\pi \text{sgn}[w] (\gamma_0 w - \boldsymbol{\gamma} \cdot \mathbf{k} + \bar{M}_{\mathbf{k}}) \mathcal{F}(w, \mathbf{k})$$

4. Some numerical results

The finite width of the quark spectral function comes from

$$\frac{1}{2\sqrt{2\pi}E_{\mathbf{k}}\Lambda} \left[\exp \left[-\frac{(w - E_{\mathbf{k}})^2}{2\Lambda^2} \right] + \exp \left[-\frac{(w + E_{\mathbf{k}})^2}{2\Lambda^2} \right] \right] \equiv \mathcal{F}(w, \mathbf{k})$$

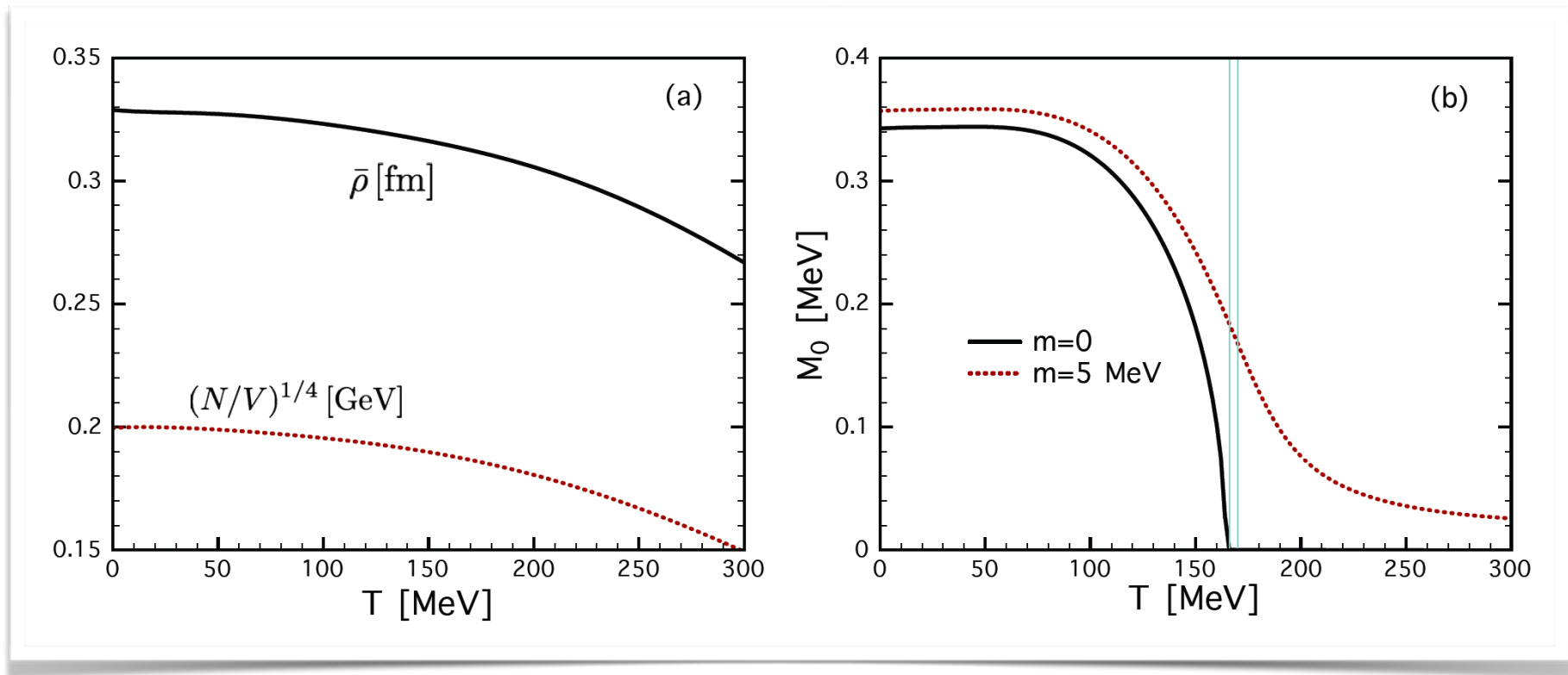
The width is taken as a model scale \sim instanton size \sim 600 MeV

Note that this function satisfies the normalization condition

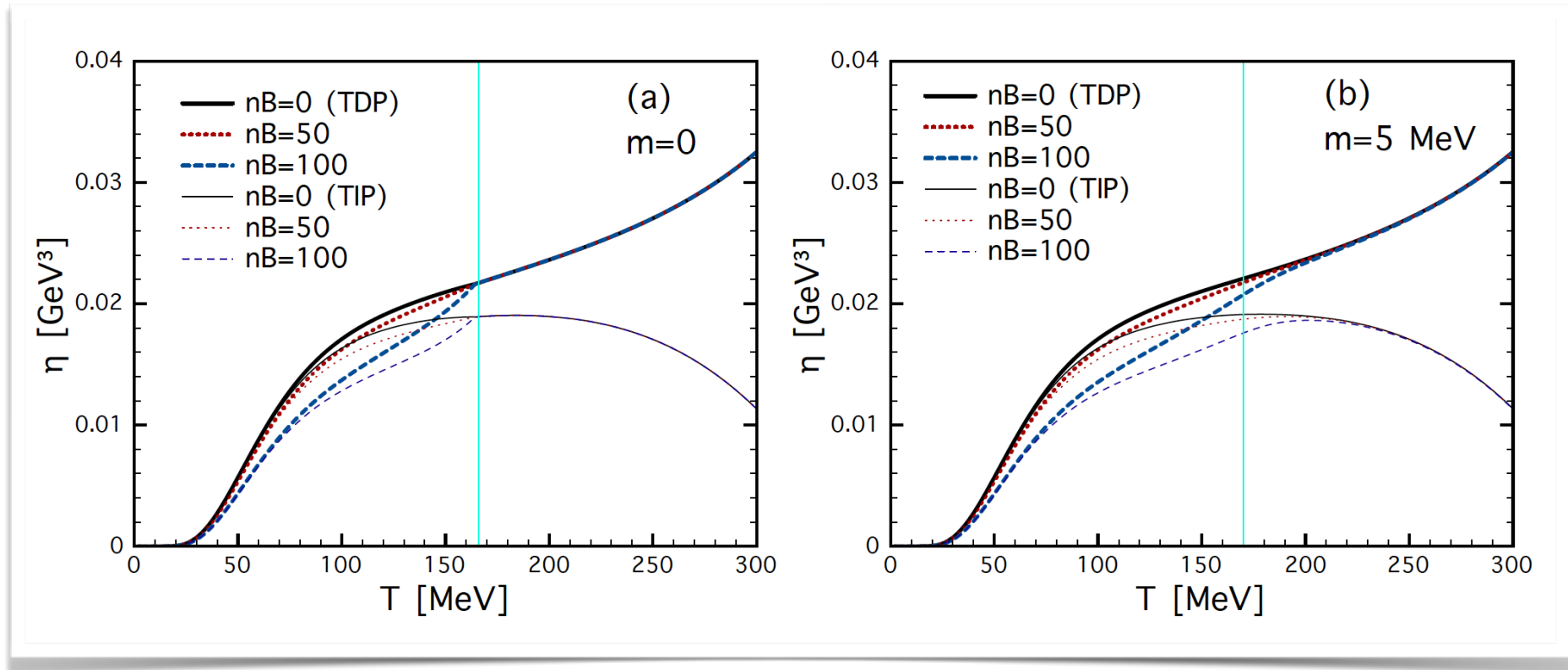
$$\frac{1}{2\pi} \int \rho(w, \mathbf{k}) dw = \gamma_0$$

Performing the trace and arithmetic calculations..

$$\eta = \frac{N_c N_f}{2\pi^2 T} \int dk_0 d^3 \mathbf{k} n_F(k_0) [n_F(k_0) - 1] \mathcal{F}^2(w, \mathbf{k}) k_x^2 [2k_y^2 + k^2 - M_{\mathbf{k}}^2]$$



4. Some numerical results

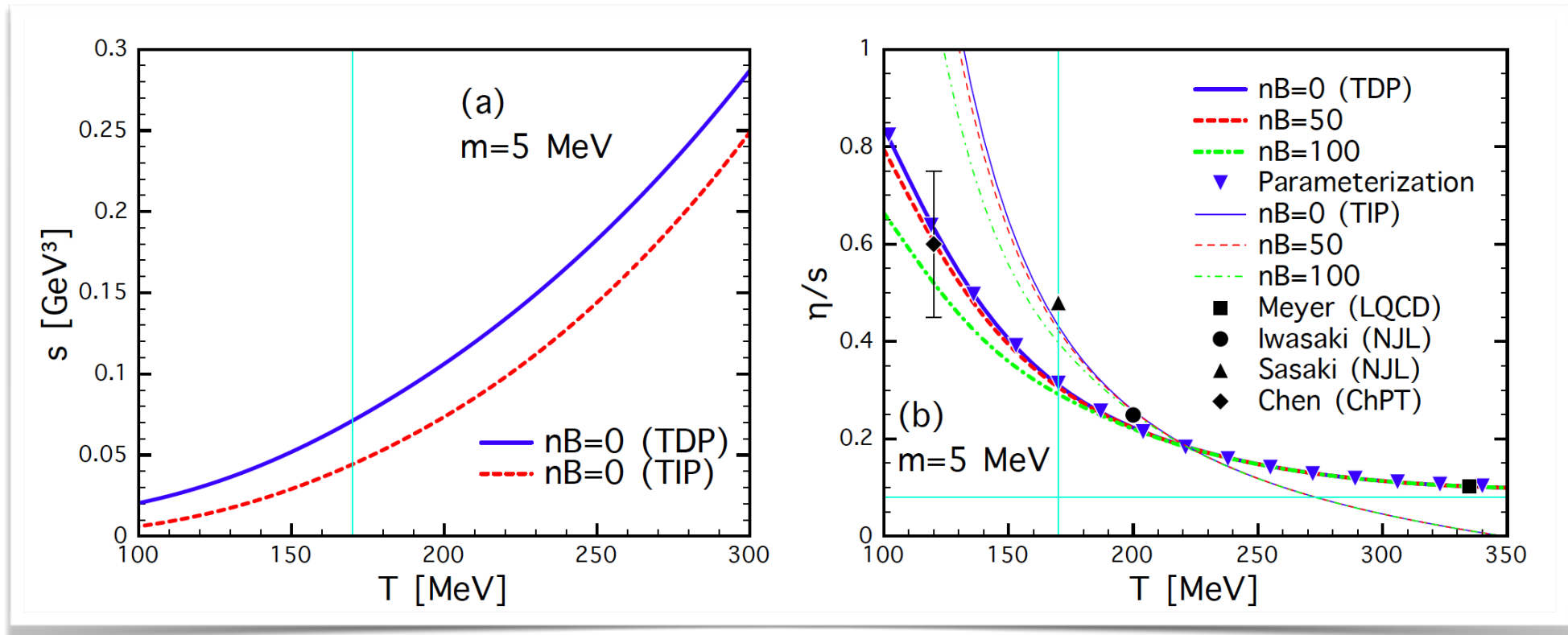


TD(I)P: Temperature (in)dependent parameters of ρ and N/V

TDP curves increase wrt T , whereas TIP ones get diminished beyond T_c .

B-field effects negligible beyond T_c : Less effects on QGP

4. Some numerical results



Entropy density shows increasing functions of T for TDP and TIP

$\text{Min}[\eta/s] \sim 1/(4\pi)$: KSS bound (Kovtun, Son, and, Starinets)

LQCD, NJL, and ChPT results are compatible with ours

Kubo formula for electric conductivity σ

- σ can be written in terms of the following vector current correlator (VCC)

$$\sigma_{\mu\nu}(p) = -\frac{1}{6w_p} \int d^4x e^{ipx} \langle [J_\mu^V(x), J_\nu^V(0)] \rangle$$

- It also connects to vector spectral function (VSF): $\sigma \sim \text{VCC} \sim \rho_V$
- In momentum space, it is evaluated into

$$\sigma_{\mu\nu}(p) = -\sum_f \frac{e_f^2}{w_p} \int \frac{d^4k}{(2\pi)^4} \text{Tr}_{c,\gamma} [S(k) \gamma_\mu S(k+p) \gamma_\nu]_A$$

SiN, Phys. Rev. D 86, 033014 (2012).

$$(e_u, e_d) = (2e/3, -e/3)$$

- Quark electric charge defined as
- w_p denotes the Matsubara frequency for σ
- Quark propagator S will be derived from an effective action
- Subscript A indicates the external EM field induced for B field

Instanton liquid model at finite T

- Employing the Matsubara formula for fermion, we get EC as follows

SiN, Phys. Rev. D86, 033014 (2012)

$$\sigma_{\mu\nu}(p) = \sum_f \frac{8e_f^2 N_c T \delta_{\mu\nu}}{w_p} \sum_n \int \frac{d^3\mathbf{k}}{(2\pi)^3} \left[\frac{\frac{k^2 + w_k(w_k + w_p)}{2} + M_k^2 - 2\tilde{M}_k^2 (e_f B_0)^2}{[k^2 + w_k^2 + M_k^2][k^2 + (w_k + w_p)^2 + M_k^2]} \right] w_k = w_n \left(1 + \frac{1}{2\tau|w_n|} \right)$$

- Summation over Matsubara frequency done analytically
- The perpendicular contribution of EC to $\mathbf{B} \sim (0,0,B_0)$ field given by

$$\sigma_{\perp} = \sum_f e_f^2 N_c \tau \left\{ \int \frac{d^3\mathbf{k}}{(2\pi)^3} F_k^2(k^2) \left[\frac{\tanh(\pi\tau E_k)}{E_k} \right] + \frac{\tau\pi}{2} \int \frac{d^3\mathbf{k}}{(2\pi)^3} F_k^2(k^2) \left[\frac{\text{sech}^2(\pi\tau E_k)}{E_k^3} \left[\frac{\sinh(2\pi\tau E_k)}{2\pi\tau} - E_k \right] \right] [M_k^2 - 4\tilde{M}_k^2 (e_f B_0)^2] \right\}$$

- The parallel contribution obtained by setting $B = 0$

Instanton liquid model at finite T

- Employing the Matsubara formula for fermion, we get EC as follows

SiN, Phys. Rev. D86, 033014 (2012)

$$\sigma_{\mu\nu}(p) = \sum_f \frac{8e_f^2 N_c T \delta_{\mu\nu}}{w_p} \sum_n \int \frac{d^3\mathbf{k}}{(2\pi)^3} \left[\frac{\frac{k^2 + w_k(w_k + w_p)}{2} + M_k^2 - 2\tilde{M}_k^2 (e_f B_0)^2}{[k^2 + w_k^2 + M_k^2][k^2 + (w_k + w_p)^2 + M_k^2]} \right] w_k = w_n \left(1 + \frac{1}{2\tau|w_n|} \right)$$

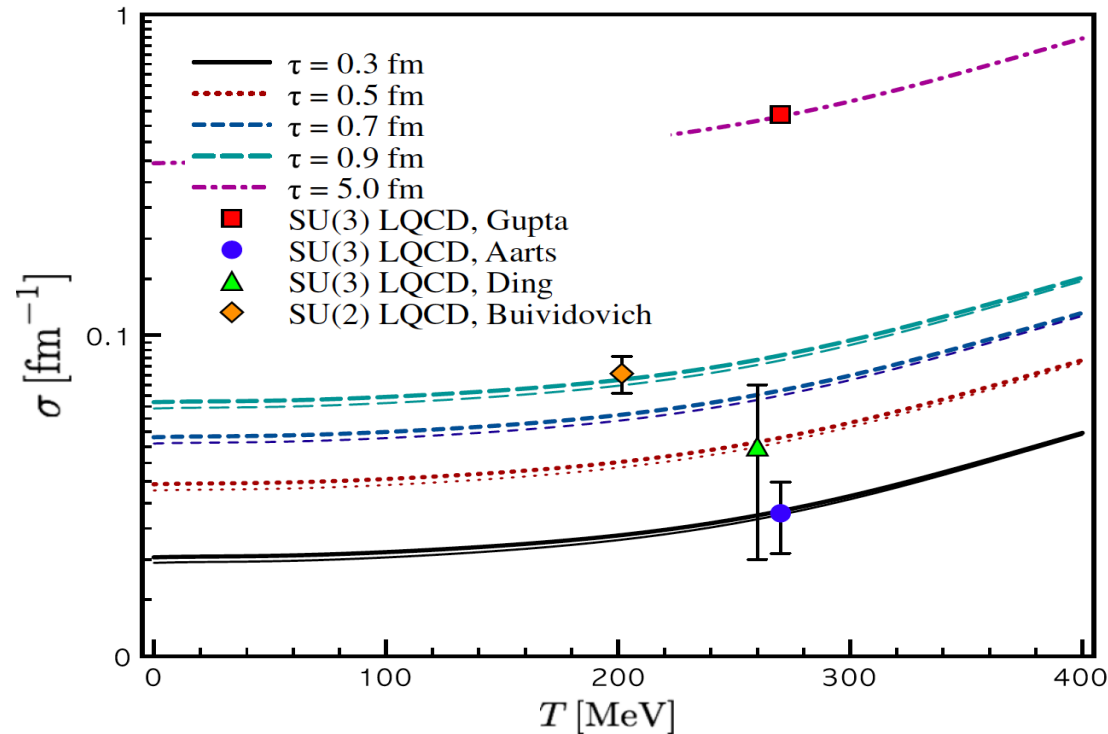
Relaxation
time

- Summation over Matsubara frequency done analytically
- The perpendicular contribution of EC to $\mathbf{B} \sim (0,0,B_0)$ field given by

$$\sigma_{\perp} = \sum_f e_f^2 N_c \tau \left\{ \int \frac{d^3\mathbf{k}}{(2\pi)^3} F_k^2(\mathbf{k}^2) \left[\frac{\tanh(\pi\tau E_k)}{E_k} \right] + \frac{\tau\pi}{2} \int \frac{d^3\mathbf{k}}{(2\pi)^3} F_k^2(\mathbf{k}^2) \left[\frac{\text{sech}^2(\pi\tau E_k)}{E_k^3} \left[\frac{\sinh(2\pi\tau E_k)}{2\pi\tau} - E_k \right] \right] [M_k^2 - 4\tilde{M}_k^2 (e_f B_0)^2] \right\}$$

- The parallel contribution obtained by setting $B = 0$

Numerical results vs. SU(Nc) lattice QCD (LQCD)



Gupta et al., PLB597 (2004)
SU(3). Unrenormalized VC

Aarts et al., PRL99 (2007)
SU(3). Unrenormalized VC

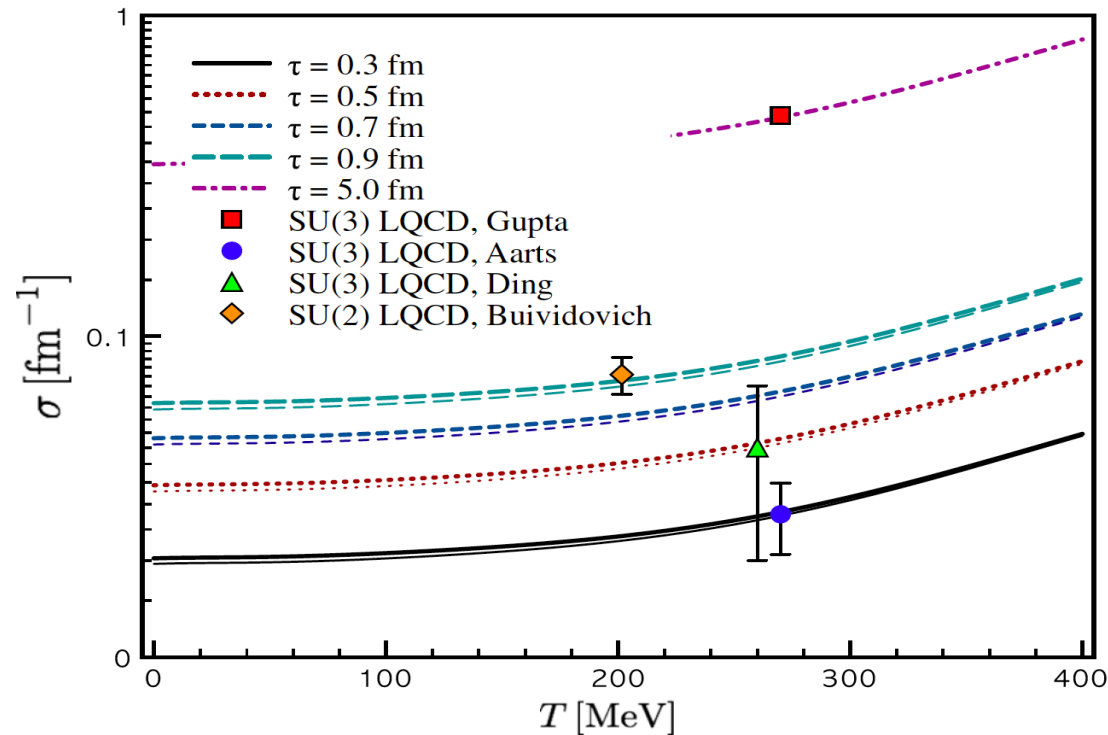
Ding et al., PRD83 (2011): SU(3)
SU(3). Unrenormalized VC

Buividovich et al., PRL105 (2010): **SU(2)**

- The numerical results compatible with LQCD data for various τ
- Effects of B field is **negligible** (thick and thin lines)
- EC increases obviously beyond $T \sim 200$ MeV

B. Kerbikov and M. Andreichikov, arXiv:1206.6044.

Numerical results vs. SU(Nc) lattice QCD (LQCD)



Gupta et al., PLB597 (2004)
 SU(3). Unrenormalized VC

Aarts et al., PRL99 (2007)
 SU(3). Unrenormalized VC

Ding et al., PRD83 (2011): SU(3)
 SU(3). Unrenormalized VC

Buividovich et al., PRL105 (2010): **SU(2)**

	$T = 0$	$T = 100$ MeV	$T = 200$ MeV	$T = 300$ MeV	$T = 400$ MeV
$\tau = 0.3$ fm	0.020	0.021	0.024	0.031	0.049
$\tau = 0.5$ fm	0.034	0.036	0.040	0.053	0.083
$\tau = 0.7$ fm	0.048	0.050	0.056	0.074	0.116
$\tau = 0.9$ fm	0.062	0.064	0.072	0.095	0.149

Numerical results vs. effective model

- EC can be parameterized practically as

$$\sigma(T) = C_{\text{EM}} \sum_{m=1} C_m T^m, \quad \frac{C_m}{\text{fm}^{m-1}} \in \mathcal{R} \quad C_{\text{EM}} = \sum_f e_f^2$$

- The numerical results for the coefficients become

	$\tau = 0.3$ fm	$\tau = 0.5$ fm	$\tau = 0.7$ fm	$\tau = 0.9$ fm
C_1	0.46	0.77	1.08	1.39
C_2 [fm]	4.00×10^{-6}	6.66×10^{-6}	9.33×10^{-6}	1.20×10^{-6}
C_3 [fm ²]	-4.87×10^{-5}	-4.87×10^{-6}	-4.88×10^{-5}	-4.88×10^{-5}

- EC is almost **linear** for wide range of T
- From effective models: $\sigma = 0.04$ [1/fm]
via Green function method at T=0 and $\tau=0.9$ fm

Ours	$T = 0$
$\tau = 0.3$ fm	0.020
$\tau = 0.5$ fm	0.034
$\tau = 0.7$ fm	0.048
$\tau = 0.9$ fm	0.062

Numerical results vs. effective model

- EC can be parameterized practically as

$$\sigma(T) = C_{\text{EM}} \sum_{m=1} C_m T^m, \quad \frac{C_m}{\text{fm}^{m-1}} \in \mathcal{R} \quad C_{\text{EM}} = \sum_f e_f^2$$

~ VSF

- The numerical results for the coefficients become

	$\tau = 0.3 \text{ fm}$	$\tau = 0.5 \text{ fm}$	$\tau = 0.7 \text{ fm}$	$\tau = 0.9 \text{ fm}$
C_1	0.46	0.77	1.08	1.39
$C_2 \text{ [fm]}$	4.00×10^{-6}	6.66×10^{-6}	9.33×10^{-6}	1.20×10^{-6}
$C_3 \text{ [fm}^2\text{]}$	-4.87×10^{-5}	-4.87×10^{-6}	-4.88×10^{-5}	-4.88×10^{-5}

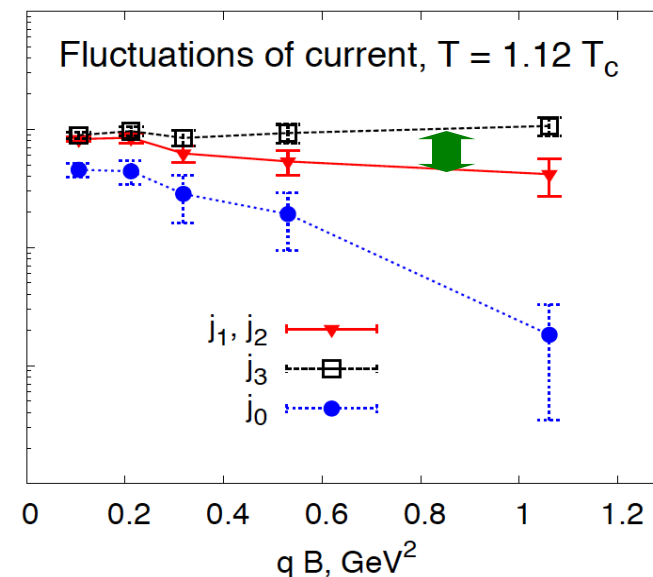
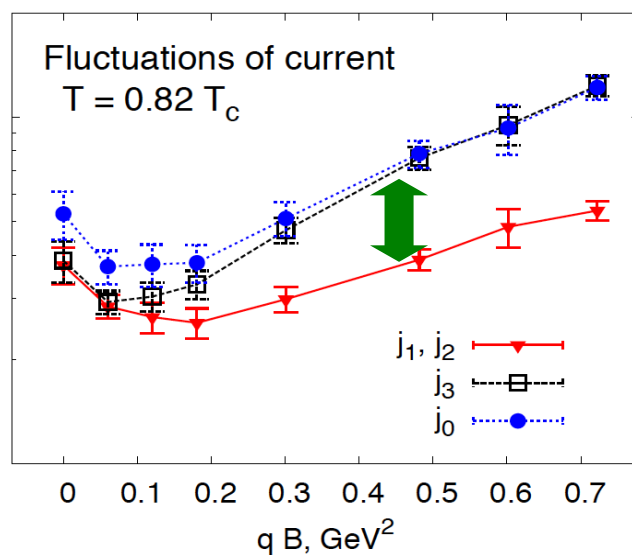
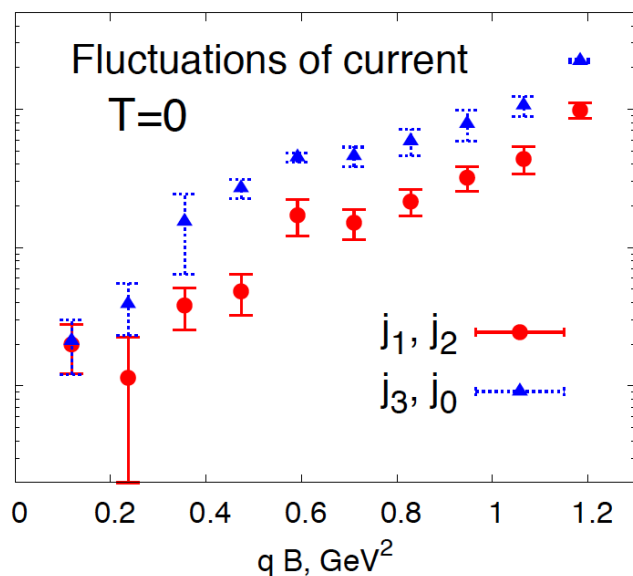
- EC is almost **linear** for wide range of T
- From effective models: $\sigma = 0.04 \text{ [1/fm]}$
via Green function method at T=0 and $\tau=0.9 \text{ fm}$

Ours	$T = 0$
$\tau = 0.3 \text{ fm}$	0.020
$\tau = 0.5 \text{ fm}$	0.034
$\tau = 0.7 \text{ fm}$	0.048
$\tau = 0.9 \text{ fm}$	0.062

A comparison to LQCD data

- EC varies significantly by B field for T in SU(2) LQCD simulation

Buividovich et al., Phys. Rev. Lett 105 (2010):



- It differs from our numerical results: negligible B-field effects
- Why?

- 1) Ignored more B-field sensitive contributions from nonzero chiral density
- 2) SU(2) LQCD data could indicate possible deviation from reality?

SiN, Phys. Rev. D 80, 114025 (2009).

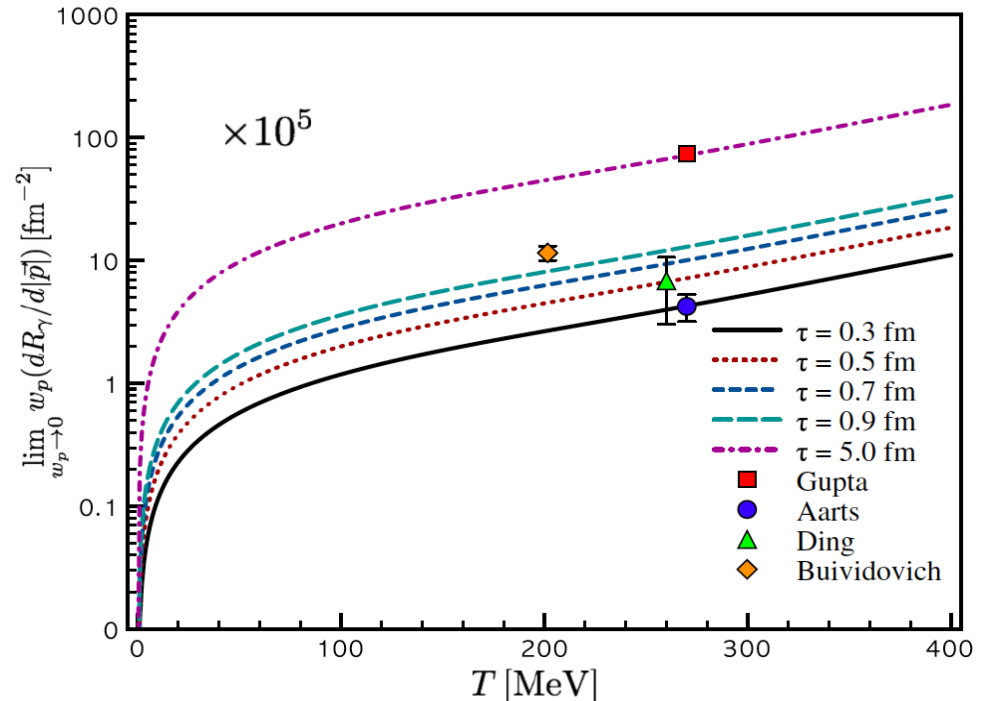
Soft-photon emission rate from EC

- Dilepton production directly related to VSF ~ VCC ~ EC

$$\mathcal{R}_\gamma \equiv \lim_{w_p \rightarrow 0} w_p \frac{dR_\gamma}{d^3|\mathbf{p}|} = \frac{3\alpha_{\text{EM}}}{2\pi^2} \sigma T.$$



Lepton pair
via virtual
photon



	$T = 100 \text{ MeV}$	$T = 200 \text{ MeV}$	$T = 300 \text{ MeV}$	$T = 400 \text{ MeV}$
$\tau = 0.3 \text{ fm}$	1.181×10^{-5}	2.700×10^{-5}	5.229×10^{-5}	11.021×10^{-5}
$\tau = 0.5 \text{ fm}$	2.024×10^{-5}	4.500×10^{-5}	8.940×10^{-5}	18.667×10^{-5}
$\tau = 0.7 \text{ fm}$	2.811×10^{-5}	6.297×10^{-5}	12.482×10^{-5}	26.089×10^{-5}
$\tau = 0.9 \text{ fm}$	3.600×10^{-5}	8.100×10^{-5}	16.025×10^{-5}	33.511×10^{-5}

5. Summary

Along with lattice QCD and theory beyond QFT, QCD-like EFT plays an important role to understand strongly-interacting systems

Strongly-interacting QGP believed to be created in HIC is a good place to test QCD in extreme conditions, i.e. hot and dense QCD matter

QCD-like EFTs are modified in medium with helps of lattice QCD, Euclidean-time formula, nonperturbative gluonic correlations, etc.

Various physical properties of QGP investigated using QCD-like EFTs, such as transport coefficients, EoS, effects of B-fields, etc.

There are still insufficient understandings and obvious distinctions between EFTs, and they can be resolved along with lattice QCD

Thank you for your attention!

This talk supported by the National Research Foundation of Korea (NRF) grant funded by the Korea government (MSIT) (No. 2018R1A5A1025563) via

Center for Extreme Nuclear Matters (CENuM)

